# Optomechanical coupling in a one-dimensional optical lattice

J. K. Asbóth,[1,2] H. Ritsch,[1] and P. Domokos[2]
[1]*Institut für Theoretische Physik, Universität Innsbruck, Technikerstrasse 25, A-6020 Innsbruck, Austria*
[2]*Research Institute of Solid State Physics and Optics, Hungarian Academy of Sciences, H-1525 Budapest P.O. Box 49, Hungary*
(Received 16 January 2008; published 30 June 2008)

In a recent paper [J. K. Asboth *et al.*, Phys. Rev. Lett. **98**, 203008 (2007)] we have shown that traveling density wavelike collective oscillations can arise in an asymmetrically pumped optical lattice, and by increasing the lattice size or pump asymmetry, these waves can destabilize the structure even in the overdamped limit. The long-range interaction giving rise to collective motion stems from the back-action of the atoms on the field creating the lattice. In this paper we present a detailed description of these phenomena. We derive the force on a disk-shaped cloud of trapped particles including the back-action on the trapping light, and analyze its relation to the standard perturbative approach giving the "dipole force" and "radiation pressure." We calculate the self-consistent lattice constant for both red and blue detuned lattices and find that it decreases—by the same amount in the two cases—as the pump asymmetry is increased. We present the detailed derivation of the lattice vibration eigenmodes using the transfer matrix method, which reveals that the instability is enhanced resonantly at certain settings of the asymmetry.

DOI: 10.1103/PhysRevA.77.063424 PACS number(s): 37.10.Jk, 37.10.Vz, 63.22.−m, 71.36.+c

## INTRODUCTION

Optical lattices (OL) are perfectly periodic arrays of particles trapped by the standing wave interference pattern of several laser beams [1,2]. OL's are created in one, two, or three dimensions, in various shapes and sizes. Whereas in the 1990s occupancies of about 1% were realistic, OL's can now be loaded from Bose-Einstein condensates and filling factors of up to 5 can be achieved [3]. OL's have important applications as model systems for solid state physics [4], for quantum information science [5], or metrology [6].

Optical lattices are generally produced using extremely far detuned lasers: detunings of about $10^7$ times the atomic transition linewidth are not uncommon. On the one hand, this ensures that the dipole force dominates the scattering force, and the particles are only slightly heated by the light used to trap them. On the other hand, in this regime the particles do not affect the propagation of light very much, and thus optical back-action is avoided. The advantage is that this way light is a tool to produce an inert potential. However, in related systems, it is the optical back-action that gives rise to useful or interesting phenomena such as cavity-induced cooling of atoms [7,8] or cooling of micromirrors [9–11].

So far, the only back-action effect seen in optical lattices is a tiny but observable reduction of the lattice constant with respect to the naive expectation (in a one-dimensional OL, this would be half of the wavelength of the trap laser $d=\frac{\lambda}{2}$). This has been predicted [12], and subsequently demonstrated [13], by Birkl *et al.*, and unambiguously observed in an experiment of Weidemüller *et al.* [14]. This phenomenon can be simply understood as a consequence of the fact that the effective wavelength of light is reduced as it has to pass through the thin cloud of trapped particles [12].

A generic physical effect due to the back-action is that the trap light mediates an interaction between the particles, which can affect the equilibrium configuration and open the possibility of collective motion. In many experimental setups this interaction is negligible, and therefore it has largely been overlooked to this day. An exception is when the trap light is spatially confined in a high-$Q$ optical resonator [15,16], where this interaction creates correlations between the motion of trapped atoms [17], and can lead to the formation of ordered structures in real space (self-organization [18–20]) or in momentum space (correlated atomic recoil laser [21–24]). Another important exception is the phenomenon of "optical binding," discovered in 1989 by Burns, Fournier, and Golovchenko [25], which has very recently attracted the attention of several groups [26–30]. The description of this phenomenon is rather involved, including the solution of multiple scattering in a two- or three-dimensional situation, and thus, analytical results are rarely found (an exception is Ref. [31]).

In this paper we study the radiative atom-atom interaction due to optomechanical coupling in the simplest possible case, a one-dimensional optical lattice in free space. Using the framework of Deutsch *et al.* [12] as a starting point, the trapped clouds of atoms will be identified with single scattering centers, i.e., beam splitters in one dimension. We derive the optical force on such a beam splitter and generalize the standard "radiation pressure" and "dipole force" [32]. These latter can be considered as perturbative approximations to our exact result, in which the back-action of the scatterer on the optical field is neglected. The exact result accounting for back-action can be interpreted by means of a simple physical picture, in terms of multiple reflection within the beam splitter.

The modification of the optical force, due to back action, on a single atom cloud is small. However, we have found that tuning a hitherto neglected parameter of an optical lattice its consequences can become striking. This parameter, the "asymmetry," is the relative power of the pump beams constituting the trap. For symmetric OL's—created by two counterpropagating beams with the same intensity—the back-action-induced interaction leads to the reduction of the lattice constant $d$ mentioned above, and we predict that it also causes the center-of-mass oscillations to soften. In asymmetric lattices, the reduction of the lattice constant $d$ is

 

enhanced (in some cases by several orders of magnitude), and arises even for blue detuning, where the first intuition would suggest that $d$ increases. However, this equilibrium phenomenon is masked by dynamic effects. The interaction induced by back-action leads to a dynamic instability of optical lattices, which happens already at moderate pump asymmetries. Small lattice fluctuations give rise to an exponentially increasing density wave propagating along the direction of the weaker beam, which ultimately leads to a destruction of the lattice: the particles will all be pushed away by the stronger beam. Viscous friction can prevent this instability, but even with an arbitrary amount of friction (overdamped limit) there is a critical asymmetry beyond which the OL becomes unstable. Curiously, the propagating density waves arise in the overdamped limit as well, in spite of the fact that the dynamics is first order. We study these effects numerically and analytically, providing an analytical characterization of the density waves and closed formulas for the critical asymmetries.

This article is organized as follows. We first introduce the model of Deutsch *et al.* [12] we use to compute the back-action of trapped particles on the trapping field, in Sec. I. Then we derive simple closed formulas for the optical forces on trapped atom clouds, using the Maxwell stress tensor, in Sec. II. We calculate the equilibrium optical lattice configuration revealing that the lattice constant is reduced if the pump asymmetry is increased in Sec. III. This effect, however, is masked by the dynamics of the lattice, which we explore using numerical simulation in Sec. IV. We characterize the vibrational modes of the lattice by a full analytical solution of the dynamics close to equilibrium in Sec. V. Although the analytical calculations are for a perfect lattice, the main features of the dynamics persist even in the presence of noise, as we illustrate in Sec. VI. We address some of the experimental issues and give estimations for the real-life values of the physical quantities involved in Sec. VII. Finally, we give an outlook and show how some of the features of dynamics arise in related systems in our conclusions.

## I. THE LIGHT IN AN OPTICAL LATTICE

We consider a one-dimensional dipole trap constituted by two counterpropagating laser beams of equal polarization and frequency, coming from the same "master laser," and thus phase stabilized with respect to each other. The transverse profile ($y$ and $z$ dependence) of the electric fields is assumed to be Gaussian, with beam diameter much larger than the wavelength $w \gg \lambda$. Thus the intensity maxima and minima are both thin disks. Suppressing the vector indices, in the usual complex notation we write the electric field incident from the left as $E(x,t)=E_0 e^{ikx-i\omega t}$ and from the right $E(x,t)=E_1 e^{-ikx-i\omega t}$. In the following, for brevity we drop the trivial phase factors $e^{-i\omega t}$. Although the two incident plane waves have the same frequency, their intensities $I_j(x) = \frac{1}{2}\epsilon_0 c|E_j(x)|^2$, for $j=1,2$, can be different—for definiteness, we choose $I_1 > I_0$. We quantify this intensity imbalance using two alternative dimensionless quantities, the normalized difference of the intensities, the pump asymmetry

$$\mathcal{A} = \frac{I_1 - I_0}{\sqrt{I_0 I_1}} > 0 \tag{1}$$

and the pump power ratio

$$\mathcal{P} = \frac{I_1}{I_0} = \frac{|E_1|^2}{|E_0|^2} = \frac{1}{4}(\mathcal{A} + \sqrt{4+\mathcal{A}^2})^2 > 1. \tag{2}$$

For almost symmetric pumping ($\mathcal{A} \ll 1$), the two are related by $\mathcal{P}=1+\mathcal{A}$, whereas for highly asymmetric pumping ($\mathcal{A} \gg 1$), roughly $\mathcal{P}=\mathcal{A}^2$.

The trap is used to hold particles, which can be (ultra)cold atoms or submicron size plastic beads, with diameter much smaller than the wavelength. For simplicity we assume linear polarizability of these particles (the dipole transitions are not saturated). The particles can be "high-field seekers": cold atoms, with the trapping light red detuned with respect to the characteristic frequency $\omega_A$ of the atomic resonance, or submicron plastic beads, where the index of refraction of the surrounding medium is lower than that of the trapped particles. In this case, the particles accumulate around the intensity antinodes. Alternatively, they can be "low-field seekers": for cold atoms, this corresponds to blue detuning of the lattice lasers $\omega < \omega_A$ for microscopic particles it means that they are surrounded by a medium with an index of refraction exceeding their own. In that case, the particles are expelled from regions where the intensity is high: if some external trap mechanism prevents their escaping the beam in the transverse $y$ and $z$ directions, they will gather around the nodes of the trapping field. In either case, we assume that the particles are cold enough and the laser beams intensive enough so that they are deeply trapped, and thus form a stack of pancake-shaped clouds. Within a single cloud, we average over transverse motion of particles, thus each cloud is represented by an infinitely thin plane of linearly polarizable material. The limits of validity of these simplifying assumptions are discussed briefly in Sec. VII.

The strength of interaction of a cloud of trapped particles with the laser depends on the linear polarizability $\alpha$ of the particles (a complex quantity), and on their areal density

$$\eta = \frac{N_\lambda}{\lambda^2} = \frac{(\text{number of particles in a cloud})}{(\text{cloud cross section})}, \tag{3}$$

with $N_\lambda$ denoting the number of atoms in a part of the cloud with area $\lambda^2$. Together these give the dimensionless complex coupling constant $\zeta$, the (areal density of the) polarizability of a cloud

$$\zeta = k\eta\frac{\alpha}{2\epsilon_0}. \tag{4}$$

The real part Re $\zeta$ describes dispersive atom-light interactions. It is positive for red detuning (of the trap laser with respect to the atomic resonance), negative for blue detuning. The imaginary part Im $\zeta$ which is always positive, corresponds to dissipation. For a detailed discussion of how $\zeta$ is related to the parameters of the trapped atoms or microbeads and the laser, see Sec. VII.

As is well known, the polarizability $\zeta$ is proportional to the optical forces that trap the particles in the lattice, which

we are going to discuss in the next section. However, it also gives the magnitude of the back-action of the cloud on the trapping light. Following Deutsch *et al.* [12], we take this effect into account by calculating the propagation of the trap light via the scalar Helmholtz equation, with the $N$ clouds represented by Dirac-$\delta$ distributions of linearly polarizable material

$$(\partial_x^2 + k^2)E(x) = -2kE(x)\sum_{j=1}^{N} \zeta\delta(x - x_j). \tag{5}$$

If the dissipative part of the light-matter interaction (spontaneous emission) can be neglected, $\zeta \in \mathbb{R}$, the Helmholtz Eq. (5) for propagation of light is identical to the Kronig-Penney model in solid state physics for the propagation of electrons. Even with dissipation, for general $\zeta \in \mathbb{C}$, the solution of Eq. (5) between two clouds is a superposition of plane waves

$$E(x_{j-1} < x < x_j) = A_j e^{-ik(x-x_j)} + B_j e^{ik(x-x_j)}$$
$$= C_{j-1} e^{-ik(x-x_{j-1})} + D_{j-1} e^{ik(x-x_{j-1})}. \tag{6}$$

Integrating Eq. (5) over $x_j$, for $j=1,\ldots,N$, reveals that the scatterers constitute boundary conditions for the field:

$$E(x = x_j - 0) = E(x = x_j + 0), \tag{7a}$$

$$\partial_x E(x = x_j - 0) = \partial_x E(x = x_j + 0) + 2k\zeta E(x_j). \tag{7b}$$

Substituting the modal decomposition (6), the boundary conditions give simple algebraic relations between the mode amplitudes to the left and to the right of each atom cloud. These have the form of beam splitter (BS) relations

$$A_j = \mathfrak{r}B_j + \mathfrak{t}C_j, \tag{8a}$$

$$D_j = \mathfrak{t}B_j + \mathfrak{r}C_j, \tag{8b}$$

with reflection and transmission coefficients [12]

$$\mathfrak{r} = \frac{i\zeta}{1 - i\zeta}, \quad \mathfrak{t} = \frac{1}{1 - i\zeta}, \quad \text{whereby} \quad \zeta = -i\frac{\mathfrak{r}}{\mathfrak{t}}. \tag{9}$$

We note that a general linear optics four-port can be described by four independent real parameters, whereas here we have only two: the real and imaginary parts of $\zeta$. The reason is that we require that the electric field be continuous at the position of the BS (infinitely thin beam splitter):

$$A + B = C + D, \tag{10}$$

which leads directly to $\mathfrak{r}+1=\mathfrak{t}$. As a result of interference the electric field is reduced at the position of the BS with respect to its expected value based on the incoming amplitudes $B$ and $C$: $A+B=C+D=\mathfrak{t}(B+C)$. As discussed in the following section, this leads to a reduction of the "dipole force" and "radiation pressure." The imaginary part of $\zeta$ describes dissipation

$$|A|^2 + |D|^2 = |B|^2 + |C|^2 - 2\ \mathrm{Im}\ \zeta|\mathfrak{t}(B + C)|^2 \tag{11}$$

and

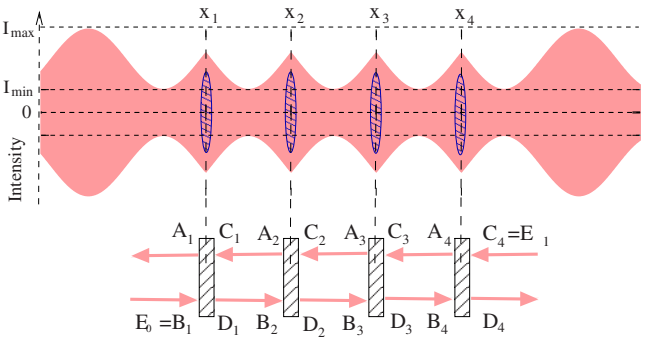


FIG. 1. (Color online) A dipole trap created by two lasers of equal frequency but unequal power. The intensity (in light red), mirrored for better visibility, ranges between $I_{\min}=\frac{1}{2}\epsilon_0 c(|E_0| - |E_1|)^2$ and $I_{\max}=\frac{1}{2}\epsilon_0 c(|E_0|+|E_1|)^2$. Trapped particles form disk-shaped clouds (in dark blue), and are modeled as beam splitters. Due to the pump asymmetry, the electric field has no nodes. Back action of trapped particles distorts the field and reduces the lattice constant.

$$|\mathfrak{r}|^2 + |\mathfrak{t}|^2 = 1 - 2|\mathfrak{t}|^2\ \mathrm{Im}\ \zeta. \tag{12}$$

For purely dispersive interaction $\zeta \in \mathbb{R}$ photon number is conserved $|\mathfrak{r}|^2+|\mathfrak{t}|^2=1$ and time inversion invariance is expressed by $\mathfrak{r}^*\mathfrak{t}+\mathfrak{t}^*\mathfrak{r}=0$. In that case, the reflection and transmission coefficients are $\mathfrak{r}=i\sin\chi_0 e^{i\chi_0}$ and $\mathfrak{t}=\cos\chi_0 e^{i\chi_0}$, with $\chi_0=\tan^{-1}\zeta$.

### The transfer matrix method

Since a single atom cloud is modeled as a beam splitter, an optical lattice consisting of several (hundreds of) such clouds can be represented by cascaded BS's, as illustrated in Fig. 1. The beam splitter relations and those for free propagation of light give $4N$ linear equations for the $4N$ mode amplitudes $A_j, B_j, C_j, D_j$, $j=1,\ldots,N$, where $E_0=B_1$ and $E_1=C_N$ are the incident electric fields. The most straightforward way to obtain the simultaneous solution of all of these equations is via the transfer matrix (TM) method, as used, e.g., in Ref. [12].

The essence of the TM method, as illustrated in Fig. 2, is that instead of relating the outgoing modes to the incoming ones, we relate the modes to the left of an optical element to the modes to the right of it. For a linear system the relationship will be linear, and thus is given by a matrix; in our case, its size is $2\times 2$. The advantage of the approach is that it is

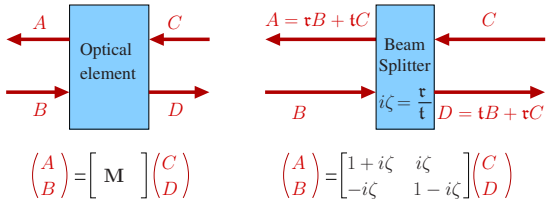


FIG. 2. (Color online) The transfer matrix relates the mode amplitudes to the left of an optical element to the mode amplitudes to the right of it. As an illustration, we give the transfer matrix of a beam splitter.

very easy to scale up a system: the TM of a composite (cascaded) system is just the matrix product of the TM's of its components.

For a single atom cloud, the BS relations (8a) and (8b) give

$$\mathbf{M}_{\mathrm{BS}} = \frac{1}{\mathfrak{t}}\begin{pmatrix} \mathfrak{t}^2 - \mathfrak{r}^2 & \mathfrak{r} \\ -\mathfrak{r} & 1 \end{pmatrix} = \begin{pmatrix} 1+i\zeta & i\zeta \\ -i\zeta & 1-i\zeta \end{pmatrix} = 1 + i\zeta\begin{pmatrix} 1 & 1 \\ -1 & -1 \end{pmatrix} = 1 + i\zeta\mathbf{B}, \tag{13}$$

with the parametrization (9) for $\mathfrak{r}$ and $\mathfrak{t}$, and the matrix $\mathbf{B}$ defined by the last equality. This can be contrasted with the TM for the corresponding incoherent scattering process, where for the intensities $A$, $B$, $C$, and $D$ we have $A=RB+TC$ and $D=RC+TB$, with $R,T>0, R+T=1$:

$$\mathbf{M}_{\mathrm{SC}} = \frac{1}{T}\begin{pmatrix} T^2 - R^2 & R \\ -R & 1 \end{pmatrix} = \begin{pmatrix} 1-\rho & \rho \\ -\rho & 1+\rho \end{pmatrix} = 1 - \rho\mathbf{B}^{\dagger}, \tag{14}$$

where $\rho=R/T$. Now $\mathbf{B}=(1;-1)^{\dagger}\circ(1;1)$ is the dyadic product of two orthogonal vectors, and thus $\mathbf{B}^2=\mathbf{B}^{\dagger 2}=0$. It follows directly that $\mathbf{M}_{\mathrm{SC}}(\rho)\mathbf{M}_{\mathrm{SC}}(\rho')=\mathbf{M}_{\mathrm{SC}}(\rho+\rho')$ and $\mathbf{M}_{\mathrm{BS}}(\zeta)\mathbf{M}_{\mathrm{BS}}(\zeta')=\mathbf{M}_{\mathrm{BS}}(\zeta+\zeta')$: two subsequent scattering processes can be represented by a single process, and the parameters $\rho$, respectively, $\zeta$, are additive. For incoherent scattering processes this relation is used to show that $\rho$ is proportional to the resistivity. For coherent scattering, however, no simple conclusions involving the "reflectivity" of a cascade of BS's can be drawn. The complication is that whereas the intensities do not change during free propagation, the amplitudes acquire phases, and in coherent processes these phases play a role. Thus it is vitally important to include the propagation of light with wave vector $k$ between BS's over length $d$ into the transfer matrix of a unit of an optical lattice

$$\mathbf{M} = \mathbf{M}_{\mathrm{BS}}\mathbf{P}(d) = \mathbf{M}_{\mathrm{BS}}\begin{pmatrix} e^{ikd} & 0 \\ 0 & e^{-ikd} \end{pmatrix} = \begin{pmatrix} (1+i\zeta)e^{ikd} & i\zeta e^{-ikd} \\ -i\zeta e^{ikd} & (1-i\zeta)e^{-ikd} \end{pmatrix}. \tag{15}$$

Due to the nontrivial propagation there is now no simple additive parameter.

We can rewrite the transfer matrix $\mathbf{M}$ into a form useful for analytical calculations, and giving the TM of a regular optical lattice instantly. For this, first note an important property of the TM of a beam splitter: reflection symmetry along $x$. By "reflection" we here refer to the exchange of the amplitudes of the left- and right-propagating components, which for the formal vector composed of the field amplitudes can be realized by multiplication by a matrix

$$\begin{pmatrix} D \\ C \end{pmatrix} = \boldsymbol{\sigma}\begin{pmatrix} C \\ D \end{pmatrix}; \quad \boldsymbol{\sigma} = \begin{pmatrix} 0 & 1 \\ 1 & 0 \end{pmatrix} \quad \text{(reflection along } x\text{)}. \tag{16}$$

As this is a reflection, $\boldsymbol{\sigma}^{-1}=\boldsymbol{\sigma}$. For a beam splitter, reflection along $x$ corresponds to the simultaneous swapping of the amplitudes $A\leftrightarrow D$ and $B\leftrightarrow C$. By Eq. (7a) and (7b), this is a symmetry of the BS relations

$$\begin{pmatrix} A \\ B \end{pmatrix} = \mathbf{M}_{\mathrm{BS}}\begin{pmatrix} C \\ D \end{pmatrix} \Leftrightarrow \begin{pmatrix} D \\ C \end{pmatrix} = \mathbf{M}_{\mathrm{BS}}\begin{pmatrix} B \\ A \end{pmatrix}, \tag{17}$$

regardless of whether the BS is purely dispersive $\zeta\in\mathbb{R}$ or there is some dissipation $\zeta\in\mathbb{C}$. Using the more concise formalism introduced above, we have

$$\boldsymbol{\sigma}\mathbf{M}_{\mathrm{BS}}\boldsymbol{\sigma} = \mathbf{M}_{\mathrm{BS}}^{-1} \quad \text{(reflection symmetry of a BS)}. \tag{18}$$

Reflection symmetry also holds for free propagation $\boldsymbol{\sigma}\mathbf{P}(d)\boldsymbol{\sigma}=\mathbf{P}(-d)$ and, therefore, also for $\mathbf{P}(d/2)\mathbf{M}_{\mathrm{BS}}\mathbf{P}(d/2)$. Due to reflection symmetry then, the product of the eigenvalues of $\mathbf{P}(d/2)\mathbf{M}_{\mathrm{BS}}\mathbf{P}(d/2)$ has to be 1. Since this TM has the same spectrum as $\mathbf{M}=\mathbf{M}_{\mathrm{BS}}\mathbf{P}(d)$, the same holds for $\mathbf{M}$: $\det\mathbf{M}=1$, and its eigenvalues can be written as $m_{\pm}=e^{\pm i\Theta}$, where $\Theta$ is a complex number [33]. The characteristic equation of $\mathbf{M}$ is $m_{\pm}^2-\mathrm{tr}\,\mathbf{M}m_{\pm}+1=0$, whose solution supplies us with the formula for $\Theta$:

$$\cos\Theta = \frac{1}{2}\mathrm{tr}\,\mathbf{M} = \cos kd - \zeta\sin kd. \tag{19}$$

We can use this result to rewrite the transfer matrix $\mathbf{M}$:

$$\mathbf{M} = \cos\Theta + i\begin{pmatrix} \zeta\cos kd + \sin kd & \zeta e^{-ikd} \\ -\zeta e^{ikd} & -\zeta\cos kd - \sin kd \end{pmatrix} = \cos\Theta + i\mathbf{A}\sin\Theta, \tag{20}$$

where the last equation defines the matrix $\mathbf{A}$. Now obviously $\mathrm{tr}\,\mathbf{A}=0$, and its eigenvectors $\mathbf{u}$ and $\mathbf{w}$ are the same as those of $\mathbf{M}$, the corresponding eigenvalues have to be $\pm1$ (to have $m_{\pm}=e^{\pm i\Theta}$). Therefore $\mathbf{A}^2=1$, and thus, as noted in Ref. [12], $\mathbf{M}=e^{i\Theta\mathbf{A}}$. For the TM of equidistant lattices, we then simply have $\mathbf{M}^N=e^{iN\Theta\mathbf{A}}=\cos(N\Theta)+i\mathbf{A}\sin(N\Theta)$. Thus, $\Theta/d$ is analogous to the Bloch quasimomentum, and Eq. (19) is the transcendental equation giving the dispersion relation of Bloch states.

## II. DIPOLE FORCE

We have described how to calculate the amplitudes of the modes inside a 1D system of optical scatterers. We now address the question of how to specify the equilibrium positions of these scatterers, more generally, what the optical forces on them are. The first issue is important since in standard textbooks the optical forces are usually derived from the dipole coupling Hamiltonian, and therefore it is tempting to identify the zero-temperature equilibrium configuration of a system with the one minimizing the dipole potential (e.g., Refs. [34–36]). However, as discussed in Ref. [37], this approach is flawed, and in the regime where the atomic back-

action is substantial, it can lead to nonphysical results. Instead of deriving the potential, we have to derive the force on the trapped particles.

The optical force on a body is the rate of the extraction of momentum from the electromagnetic field due to the presence of the body. To quantify this, we can enclose the body in a fictitious "box" and integrate the momentum flux (the Maxwell stress tensor) on the boundary of this box, as, e.g., in Ref. [38]. For the planar atom clouds in our 1D model this is very easily done. For a selected atom cloud, we take the surface around it to consist of two planes orthogonal to the $x$ axis, between the atom cloud and the two neighboring clouds. As the electromagnetic wave is transverse, both the **E** and **B** vectors lie in the planes, and the only part of the stress tensor contributing to the integral is the term with the energy density. For the plane waves of Eq. (6) this results in a simple formula for the areal density $F$ of the optical force (the force divided by the transverse area, with dimensions of pressure) on a cloud

$$F = \frac{\epsilon_0}{2}(|A|^2 + |B|^2 - |C|^2 - |D|^2). \tag{21}$$

Although the simple formula (21) for the force is very practical for both numerical and analytical work, we can gain more insight into the physics it represents by rewriting it to show its position dependence explicitly. Taking incident field amplitudes $B(x)=E_0e^{ikx}$ and $C(x)=E_1e^{-ikx}$, the BS relations of Sec. I supply us with the outgoing amplitudes $A(x)$ and $D(x)$, which can be substituted into Eq. (21) to give

$$F(x) = 2\frac{I_0 - I_1}{c}\frac{\mathrm{Im}\,\zeta}{|1-i\zeta|^2} - 4\frac{\sqrt{I_0 I_1}}{c}\frac{\mathrm{Re}\,\zeta}{|1-i\zeta|^2}\sin(2kx+\varphi) + 2\frac{I_0 - I_1}{c}\frac{|\zeta|^2}{|1-i\zeta|^2}, \tag{22}$$

where $\varphi = \arg B(x=0) - \arg C(x=0)$ is the relative phase of the two incident trapping beams at $x=0$. For low density or weak polarizability $|\zeta| \ll 1$, the force is typically dominated by the first two terms. To first order in $\zeta$, these arise from the standard microscopic light-induced forces [32] acting on each scatterer independently. To apply the model of Ref. [32], we assume large detuning from the atomic resonances and low saturation of the dipoles (linear regime). Then if we neglect the back-action of the particles on the light, each of them experiences the electric field $E(x)=E_0e^{ikx}+E_1e^{-ikx}$, and we can directly apply the formulas from Ref. [32] giving the "dissipative" and "reactive" part of the mechanical effects of light. This reproduces the first two terms of Eq. (22), apart from the factors of $|1-i\zeta|^{-2}$. Thus the formula (22) for the force can be seen as a generalization of the standard theory for light-induced forces to the regime where it is not enough to account for the effect of the dipoles on the electric field only perturbatively. Alternatively, if the individual dipoles interact weakly with the field—which is the standard case for trapped ultracold atoms—Eq. (22) can be derived from the microscopic forces, and thus embodies the effects of multiple scattering within the cloud, similarly to the Lorentz-Lorenz formula. We present this derivation in Appendix A.

The first term of Eq. (22) embodies a part of "radiation pressure" arising due to absorption of light in the cloud. It is proportional to the difference of the incident photon fluxes, and always gives a force pointing toward the weaker source [39]. The second term, using the terminology of Ref. [32], is up to the factor of $|1-i\zeta|^{-2}$ the density of the reactive or "dipole" force, also referred to as "gradient force." It arises due to the interference of reflected and transmitted light, i.e., absorption of photons from one trap beam and stimulated emission into the other one. As expected, for $\mathrm{Re}\,\zeta>0$, the gradient force attracts particle clouds toward areas of high intensity, for $\mathrm{Re}\,\zeta<0$, it expels the clouds from such regions. The third term can be rewritten as $c^{-1}(2|\mathfrak{r}|^2I_0 - 2|\mathfrak{r}|^2I_1)$, revealing that it is due to the incoherent reflection of the photons off the atom cloud, i.e., taking reflection into account without the effects of interference (which are supplied by the second term). This third term is proportional to the square of the polarizability $|\zeta|^2$ and thus is usually negligible for single atoms. However, in dense atom clouds, it can be of the order of, or much larger than, the first two terms.

For a single trapped cloud, we can always construct a potential by simply integrating the force (22): $V(x) = -\int_0^x F(x')dx'$. As this can be useful to understand the possibilities of trapping with two beams of different intensities, we plot it, along with some of its naïve approximations, for a specific example in Fig. 3. However, as soon as two or more clouds are trapped by the same field, their back-action on the field creates an effective interaction between them, and this potential cannot directly be applied. One might expect that a potential can be constructed that takes the interaction into account as well (as for atoms trapped in a high-$Q$ cavity [17]), but, as we find later, in Sec. V, this turns out not to be the case. In an asymmetric dipole trap, no potential can be constructed that supplies the dynamics of several trapped clouds.

Clearly the force (22) describes a sequence of (asymmetric) potential wells in one dimension if the intensity difference of the beams is so small that the dipole force (second term) dominates the scattering forces (first and last terms). A cloud can be trapped at the origin, $x=0$, if

$$\sin\varphi = -\frac{1}{2}\mathcal{A}\frac{|\zeta|^2 + \mathrm{Im}\,\zeta}{\mathrm{Re}\,\zeta}, \quad \cos\varphi = \pm\sqrt{1 - \frac{\mathcal{A}}{\mathcal{A}_{\max}}}, \tag{23}$$

where $\pm$ is "+" for red detuning $\zeta>0$ and "−" for blue detuning $\zeta<0$ and

$$\mathcal{A}_{\max} = 2\left|\frac{\mathrm{Re}\,\zeta}{|\zeta|^2 + \mathrm{Im}\,\zeta}\right| \tag{24}$$

is the maximum of the asymmetry for trapping along $x$; for $\mathcal{A} > \mathcal{A}_{\max}$ there are no traps. Thus a BS which is illuminated by mutually coherent laser beams from the two sides can be at equilibrium even if the lasers have unequal intensities, but only if $\mathcal{A} < \mathcal{A}_{\max}$ (see Ref. [40] for a similar analysis of the gradient force counteracting the dissipative force). In the purely dispersive case, i.e., if the imaginary part of $\zeta$ can be neglected [$\mathrm{Im}\,\zeta \ll (\mathrm{Re}\,\zeta)^2$], the relation (24) assumes the simple form

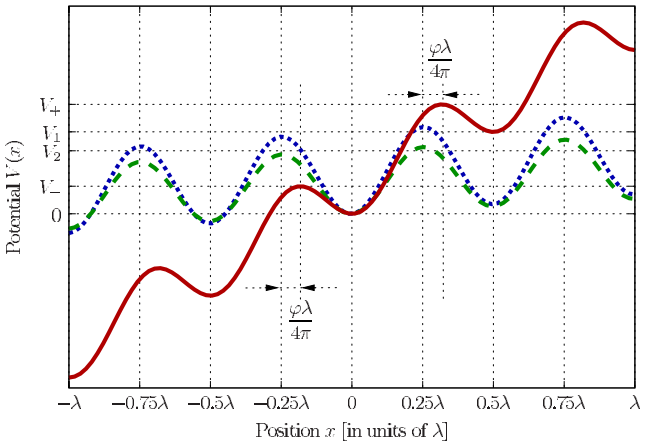


FIG. 3. (Color online) Potential of the force for a single trapped cloud, with polarizability $\zeta=0.5+0.025i$, incident intensities $I_1=4I_0$. Dotted (blue) line: potential obtained by integrating the sum of the microscopic forces, the "dipole force," and the "radiation pressure" [32] on the particles in the cloud, neglecting the change of the mode amplitudes due to the atoms. The depth of the resulting sinusoidal potential is $V_1=4\,\mathrm{Re}\,\zeta\sqrt{I_0 I_1}/\omega$, slightly decreased (increased) to the left (right) by $\pi\,\mathrm{Im}\,\zeta(I_1-I_0)/\omega$. Slashed (green) line: potential obtained by including the factors of $|1-i\zeta|^2$, accounting for the decrease of the intensity inside the clouds (similarly to the Lorentz-Lorenz formula). For these parameters this amounts to a reduction of the potential depth by 20%. Continuous (red) line: the correct potential, defined as $V(x)=-\int_0^x F(x')dx'$ with the force calculated via the Maxwell stress tensor, Eq. (22). In addition to the decrease of the potential depth, this correctly accounts for the mechanical effects of reflected light, including the third term of Eq. (22). This decreases (increases) the potential height to the left (right) by approximately $\pi|\mathrm{t}|^2(I_1-I_0)/\omega$.

$$\zeta\mathcal{A}<2, \quad \mathcal{A}_{\max}=2/\zeta, \quad \zeta_{\max}=2/\mathcal{A}. \tag{25}$$

This criterion can be intuitively understood in the following way. If $|E_0|^2<|E_1|^2$, more photons are incident on the right of the BS than the left, giving a force on it. If enough light is transmitted ($|\mathrm{t}|>\frac{1}{2}|\mathrm{r}|\mathcal{A}$), and the interference is favorable (depending on the position of the BS), the imbalance in the outgoing number of photons is enough to counteract this force, leading to a steady state.

### Equilibrium of a single cloud

The simple and very sugggestive formula (21) for the mechanical effects of light can be used to make statements about objects which are only acted on by optical forces and are at equilibrium. Since the force (21) has to vanish,

$$|A|^2+|B|^2=|C|^2+|D|^2 \quad \text{(force vanishes)}. \tag{26}$$

Furthermore, due to the possibility of dissipation inside the object, we have

$$|A|^2+|D|^2\le|B|^2+|C|^2 \quad \text{(dissipation)} \tag{27}$$

Together, these relations give

$$|A|\le|C| \quad \text{and} \quad |B|\le|D|, \tag{28}$$

with equality if $\mathrm{Im}\,\zeta=0$. When passing through the object, both beams lose in intensity, this loss is proportional to $\mathrm{Im}\,\zeta$. For purely dispersive interaction ($\zeta\in\mathbb{R}$), the intensities of the beams are unchanged.

Although in this one-dimensional setting the presence of an optically trapped purely dispersive BS cannot be inferred by observing the intensities of the transmitted light, the BS does alter the phases of the fields. Consider a single trapped pancake-shape atom cloud modeled as infinitely thin sheet of nondissipative polarizable material. At equilibrium, $\arg(A+B)=\arg(C+D)$ leads via Eq. (28) to $\arg A+\arg C=\arg B+\arg D$. For the two relative phases $\chi=\arg D-\arg C$ and $\varphi=\arg B-\arg C$ we then find, using $|A+B|=|C+D|$:

$$\sin\varphi_\pm=-\frac{1}{2}\zeta\mathcal{A}, \quad \cos\varphi_\pm=\pm\frac{1}{2}\sqrt{4-\zeta^2\mathcal{A}^2}, \tag{29}$$

$$\sin\chi_\pm=\frac{\zeta\sqrt{4+\mathcal{A}^2}\pm\zeta\sqrt{4-\zeta^2\mathcal{A}^2}}{2(1+\zeta^2)},$$

$$\cos\chi_\pm=\frac{-\zeta^2\sqrt{4+\mathcal{A}^2}\pm\sqrt{4-\zeta^2\mathcal{A}^2}}{2(1+\zeta^2)}. \tag{30}$$

Here, the "±" refers to "+" ("−") being stable and "−" ("+") being unstable equilibrium for red (blue) detuning. Clearly, Eq. (29) is just Eq. (23) rewritten for $\zeta\in\mathbb{R}$. The angle $\varphi$ shows the effect of the "back-action" force directly: for symmetric pumping and red (blue) detuning, it is zero ($-\pi$), and if $I_1$ is increased with respect to $I_0$, it increases too, showing that the atom cloud has been pushed by the "back-action" force. Since both the trap depth and this "push" are independent of the sign of $\zeta$, we have $\varphi(\zeta,\mathcal{A})-\varphi(\zeta,\mathcal{A}=0)=\varphi(-\zeta,\mathcal{A})-\varphi(-\zeta,\mathcal{A}=0)$. It is not so intuitive, but follows directly from Eq. (30) that the change in $\chi$ due to asymmetry is also insensitive to the sign of the detuning: $\chi(\zeta,\mathcal{A})-\chi(\zeta,\mathcal{A}=0)=\chi(-\zeta,\mathcal{A})-\chi(-\zeta,\mathcal{A}=0)$.

Finally we can calculate the phase slip $\Delta\phi$ of the intensity function at the position of the BS:

$$2/(\epsilon_0 c)\times I_{\mathrm{left}}(x)=|A(x)+B(x)|^2=|C|^2+|B|^2+2|BC|\cos(2kx-\chi), \tag{31}$$

$$2/(\epsilon_0 c)\times I_{\mathrm{right}}(x)=|C(x)+D(x)|^2=|C|^2+|B|^2+2|BC|\cos(2kx+\chi). \tag{32}$$

We can read off $\Delta\phi=2\chi$.

## III. SELF-CONSISTENT LATTICE CONSTANT

The result of Eq. (28) obtained in the previous section implies that in any one-dimensional structure held together by monochromatic light, with no other types of (external or interaction) forces present except for those from the purely

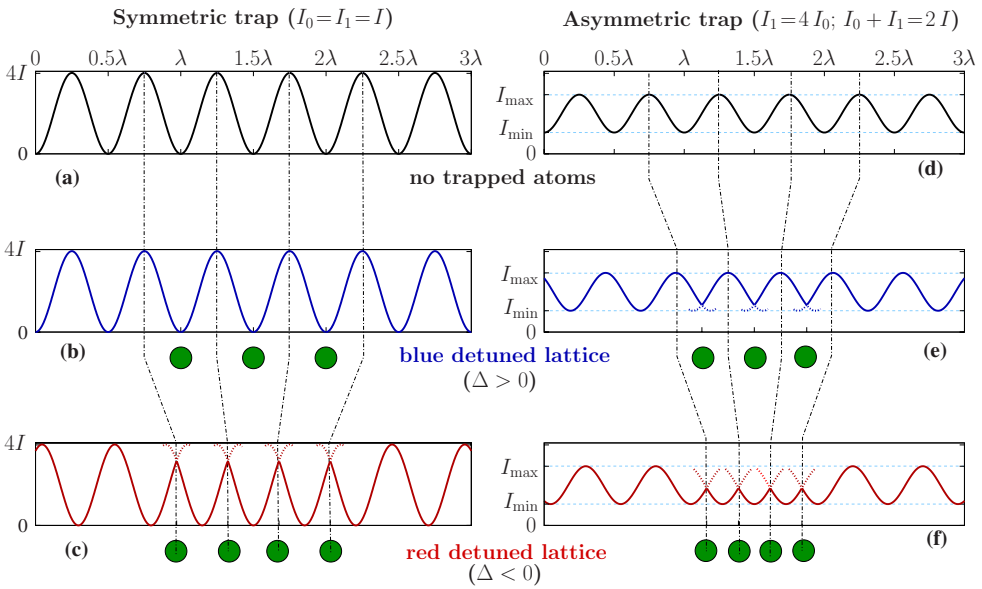


FIG. 4. (Color online) Back action of trapped particles (e.g., atoms) on the intensity of light constituting an optical dipole trap. Top line: the empty trap, created by two counter-propagating beams with equal (a) or unequal (d) intensity. In the asymmetric trap, the intensity ranges between $I_{\min}=(\sqrt{I_1}-\sqrt{I_0})^2$ and $I_{\max}=(\sqrt{I_1}+\sqrt{I_0})^2$. The total power is the same for both traps ($I_0+I_1=2I$). Middle line: blue detuning. For symmetric pumping (b), the trapped atoms sit in the dark and have no effect on the lattice. For asymmetric pumping (e), destructive interference between the trap beams cannot be perfect, and thus the atoms are polarized. As a result, the trap contracts. Bottom line: red detuning. The lattice constant is reduced in both symmetric (c) and asymmetric (f) trap, but this reduction is enhanced by the asymmetry.

dispersive dipole interaction with the trap light, the light permeates the structure unattanuated. This is a generalization of the finding of Deutsch *et al.* [12], who have shown that light permeates a regular lattice unattanuated. In formulas, at equilibrium

$$|A_1| \le |A_2| \le \cdots \le |A_N| \le |C_N| = |C|, \tag{33}$$

$$|B| = |B_1| \ge |B_2| \ge \cdots \ge |B_N| \ge |D_N|, \tag{34}$$

with equality if and only if $\zeta_1,\ldots,\zeta_N \in \mathbb{R}$. Although one might expect that due to disorder, light would be localized in a 1D lattice, this is not so if it is the light which creates the lattice itself is considered. The random variation of the coupling constants $\zeta$ causes a random variation of the lattice constant, the two types of disorder are obviously correlated. For the propagation of the light creating the lattice, either of these noises alone would localize light, but they combine to ensure that the trap light is not localized at all.

Now consider the steady state of $N>1$ identical, purely dispersive trapped clouds, with $\zeta_1=\ldots=\zeta_N=\zeta<2/\mathcal{A}$. Since at every cloud $|C_j/B_j|-|B_j/C_j|=\mathcal{A}$, the phase slips are all equal: $\chi_1=\ldots=\chi_N=\chi$. Thus the equilibrium configuration is an equidistant lattice $x_j=x_j^{(0)}=x_1^{(0)}+(j-1)d$. The lattice constant $d$ is clearly independent of $N$, and from $\Delta\phi=2\chi$, we find explicitly

$$\text{red detuning,}\quad \zeta>0:\quad d(\zeta,\mathcal{A}) = \frac{\lambda}{2}\left(1-\frac{\chi(\zeta,\mathcal{A})}{\pi}\right),$$

$$kd = \pi - \chi, \tag{35a}$$

$$\text{blue detuning,}\quad \zeta<0:\quad d(\zeta,\mathcal{A}) = \frac{\lambda}{2}\left|\frac{\chi(\zeta,\mathcal{A})}{\pi}\right|,\quad kd = -\chi. \tag{35b}$$

For symmetric pumping $\mathcal{A}=0$, we recover the results of Deutsch *et al.* [12]: for blue detuning $d(\zeta<0,\mathcal{A}=0)=\lambda/2$, whereas for red detuning we have $d(\zeta>0,\mathcal{A}=0)=d_{\text{symm}}(\zeta)=\frac{\lambda}{2}[1-2\tan^{-1}(\zeta)/\pi]$. For a given $\zeta$, increasing the pump asymmetry $\mathcal{A}$ causes the phase shift $\chi$ to increase, and $d$ to be reduced; this extra reduction turns out to be exactly the same for both red and blue detuning. Contraction of a blue detuned lattice is somewhat counterintuitive. Naively one could expect the wavelength of the trap light to be increased due to the trapped particles as it happens if the particle positions are random. For symmetric pumping, as noted in Ref. [12], the equilibrium positions of the particles are exactly at the antinodes, where they do not interact with the field, and thus do not affect the wavelength. For asymmetric pumping, we find that near the intensity minima the atoms decrease the effective wavelength, as illustrated in Fig. 4. Near the intensity maxima however, their effect is to increase the wavelength by such a large amount that for randomly positioned atoms the expected effective increase of the light passing through the gas is recovered.

The reduction of the lattice constant resulting from the pump asymmetry is shown in Fig. 5 (thick red lines). For $\mathcal{A}>2/\zeta$, the inequality (25) is violated, the stronger beam pushes all the particles away: thus the thick (red) lines in the figure all terminate at $\mathcal{A}=2/\zeta$. For red detuning, the lattice constant at this critical asymmetry is, remarkably, exactly half of its value at symmetric pumping: $d(\zeta>0,\mathcal{A}=2/\zeta)$

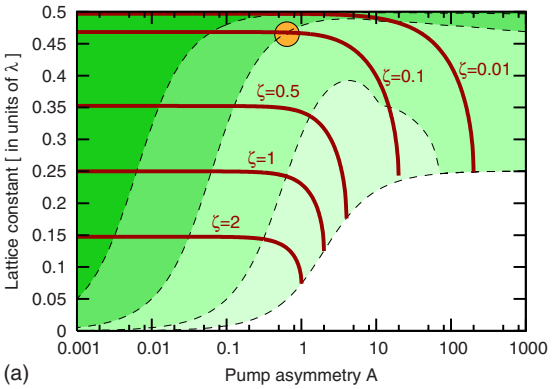


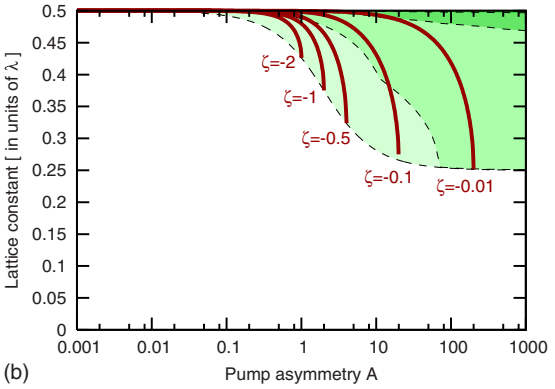


FIG. 5. (Color online) The lattice constant as a function of the asymmetry is shown in thick (red) curves for red detuning in (a) and blue detuning in (b). Shaded (green) areas indicate regions of stability for $N \leq 1000$ (darkest shade), $N \leq 100$, $N \leq 10$, and $N \leq 2$ (lightest shade). The white area is unstable, see Eq. (25). The (orange) circle in (a) marks the parameter regime of Figs. 9 and 10.

$= \frac{1}{2} d_{\mathrm{symm}}(\zeta)$, a decreasing function of $\zeta$. For blue detuning, the critical lattice constant $d(\zeta < 0, \mathcal{A} = 2/\zeta)$ increases with increasing $\zeta$.

## IV. DYNAMICS OF THE LATTICE

We have found the interesting phenomenon that back-action related effects can be enhanced by using an optical lattice where the trapping beams have unequal intensities. The next step is to investigate this situation in a computer simulation.

### Numerical simulation, overdamped dynamics

Numerical simulation of the dynamics of the optical lattice is quite straightforward. Given the positions and velocities of the $N$ atom clouds, the electric fields to the right and to the left of any cloud can be computed by the transfer matrix Method, as outlined in Sec. I. Having obtained the mode amplitudes, the optical force on all clouds is given by Eq. (21). The dynamics of the lattice is then given by a set of second-order ordinary differential equations

$$m\ddot{x}_j = -\mu x_j + F_j(x_1, \ldots, x_N) \quad \text{for} \quad j = 1, \ldots, N. \tag{36}$$

In addition to the optical forces, we have also included viscous friction with coefficient $\mu$ (related to the single-particle friction coefficient $\mu_A$ by $\mu = \eta \mu_A$) to the system: this should stabilize the optical lattice. In experiments with cold atoms in vacuum, this can correspond to some laser cooling mechanism, whereas for plastic beads immersed in water, $\mu$ follows from the Stokes law.

Before discussing the simulation results, we digress on the time scales in this dynamical system and introduce the overdamped limit. Without damping, the characteristic time scale of the cloud dynamics is given by the oscillation period of deeply trapped clouds. From formula (22) for the force, it can be seen that for small displacements $|x| \ll \lambda$, trapped clouds experience a harmonic restoring force $F = z_{\mathrm{single}} x$, where

$$z_{\mathrm{single}} = -\beta \frac{|\cos\varphi|}{|1 - i\zeta|^2} \quad \text{with} \quad \beta = 8\frac{k}{c}|\mathrm{Re}\ \zeta| \sqrt{I_0 I_1}, \tag{37}$$

and $\cos\varphi$ is given by Eq. (29). Thus the oscillation frequency of a single trapped cloud is

$$\omega_{\mathrm{single}} = \omega_{\mathrm{osc}} \frac{\sqrt{|\cos\varphi|}}{|1 - i\zeta|} \quad \text{with} \quad \omega_{\mathrm{osc}} = \sqrt{\frac{\beta}{m}}. \tag{38}$$

For low asymmetries, $\mathcal{A} \ll \mathcal{A}_{\max}$, where $|\cos\varphi| \approx 1$, and weak coupling, $|\zeta| \ll 1$, whereby $|t|^2 \approx 1$, we have $\omega_{\mathrm{single}} \approx \omega_{\mathrm{osc}}$, and the characteristic time scale of undamped cloud motion is the oscillation period of a single trapped cloud

$$\tau_{\mathrm{osc}} = 2\pi \sqrt{\frac{m}{\beta}}. \tag{39}$$

Due to the viscous friction, the velocity relaxes toward the value $F/\mu$ exponentially in time scale

$$\tau_{\mathrm{vel}} = \frac{m}{\mu}, \tag{40}$$

as can be seen by setting $F$ to a constant in Eq. (36). For small damping, this time scale exceeds $\tau_{\mathrm{osc}}$ by far ($\tau_{\mathrm{vel}} \gg \tau_{\mathrm{osc}}$), and we expect the system to perform many oscillations before the mechanical energy is totally dissipated. On the other hand, if $\tau_{\mathrm{vel}} \ll \tau_{\mathrm{osc}}$, the system is overdamped: the clouds reach the velocity $F/\mu$ in the short time scale of $\tau_{\mathrm{vel}}$, and then, on longer time scales, their motion can be described by the first-order equation obtained by dropping the inertial term of Eq. (36):

$$\mu\dot{x}_j = +F_j(x_1, \ldots, x_N) \quad \text{for} \quad j = 1, \ldots, N. \tag{41}$$

For harmonically trapped clouds, using Eqs. (22), (37), and (41), we can expect them to relax to the equilibrium positions at the bottom of their respective traps exponentially during time

$$\tau_d = \frac{\mu}{\beta}. \tag{42}$$

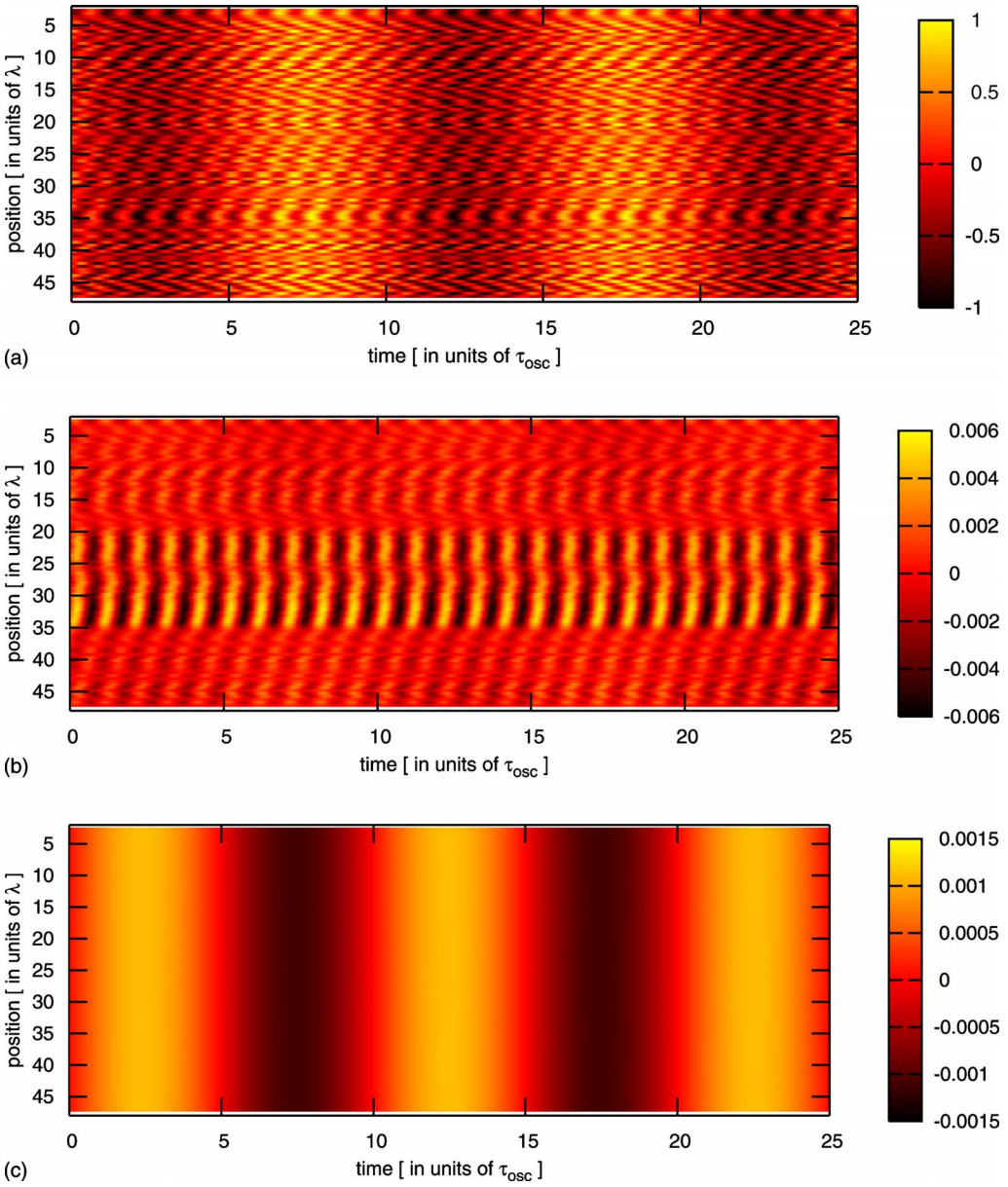


FIG. 6. (Color online) Numerical simulation of the dynamics of an optical lattice of $N=100$ clouds with polarizability $\zeta=0.1$ each, with symmetric pumping $I_0=I_1$, after initial excitation (random displacement from the equilibrium with maximum magnitude $\xi_{\text{initial}}=5\times10^{-4}\lambda$ and random velocity of maximum magnitude $\omega_{\text{osc}}\xi_{\text{initial}}$). No friction forces are assumed ($\mu=0$). Color coding stands for position distortions $\xi$ in (a), excess intensity $I(x)-(I_0+I_1)$ in (b), and excess pump asymmetry $I_{\text{left}}(x)/I_{\text{right}}(x)-I_1/I_0$ in (c).

For consistency, we can check if during time $\tau_{\text{vel}}$ the variation of the force, $dF=v\tau_{\text{vel}}(dF/dx)$ is really small for $v=F/\mu$ and $F=-\beta x$. From $dF=F\beta m/\mu^2 \ll F$ we obtain the condition that we are in the overdamped limit if

$$\beta m \ll \mu^2; \quad \text{equivalently} \quad \tau_{\text{vel}} \ll \tau_d \quad \text{or} \quad \tau_{\text{osc}} \ll \tau_d. \tag{43}$$

The last condition is equivalent to the first two because $\tau_{\text{osc}}=2\pi\sqrt{\tau_{\text{vel}}\tau_d}$. In fact, for plastic beads trapped in water, the experiments are typically in this overdamped regime (see Sec. VII for more details).

For the moment, we consider the dynamics of perfectly identical and purely dispersive clouds ($\zeta_1=\zeta_2=\ldots=\zeta_N\in\mathbb{R}$) with no dynamical noise. This first step toward understanding the dynamics of real optical lattices already provides important surprises. In any realistic simulation, absorption and noise also have to be considered. Inclusion of absorption amounts to setting $\text{Im}\,\zeta>0$. To include dynamical noise, Langevin terms need to be added to Eq. (36) and (41). To account for the uncertainty in the number of particles per cloud, we have to have $\zeta_1\neq\zeta_2\neq,\ldots,\neq\zeta_N$. We address these questions later, in Sec. VI.

We explore the dynamics of optical lattices by slightly perturbing the equilibrium and using numerical simulation to find how the system reacts. Specifically, we fix the cloud polarizabilities $\zeta$, the pump asymmetry $\mathcal{A}$, and set up a lattice configuration

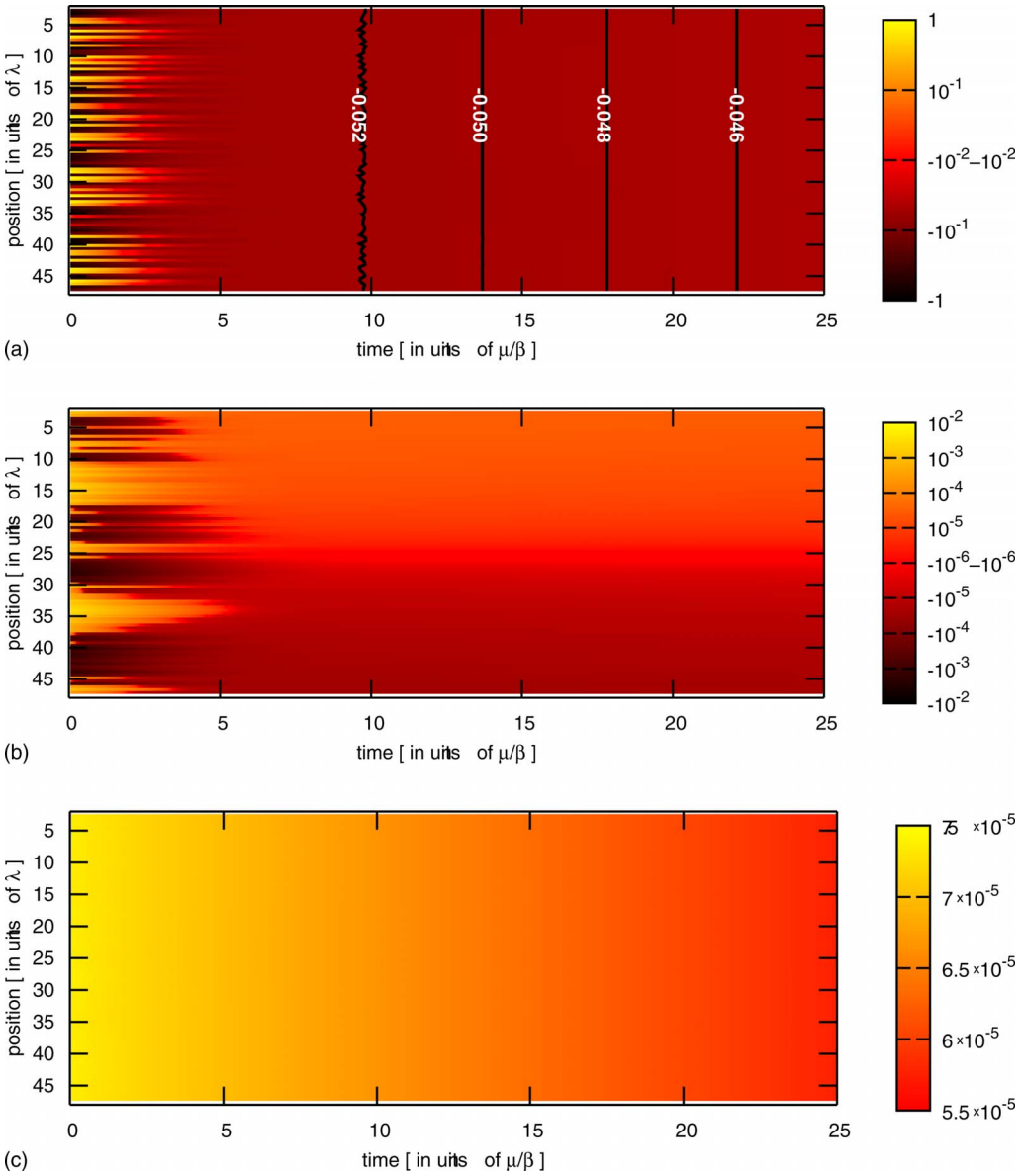


FIG. 7. (Color online) Numerical simulation of the dynamics of an optical lattice of $N=100$ clouds with polarizability $\zeta=0.1$ each, with symmetric pumping $I_0=I_1$, after initial excitation (random displacement from the equilibrium with maximum magnitude $\xi_{\text{initial}}=5\times10^{-4}\lambda$). The overdamped limit is assumed ($\mu^2 \gg \beta m$). Color coding stands for position distortions $\xi$ in (a), excess intensity $[I(x)-(I_0+I_1)]$ in (b), and excess pump asymmetry $[I_{\text{left}}(x)/I_{\text{right}}(x)-I_1/I_0]$ in (c).

$$x_j^{(0)} = x_1^{(0)} + (j-1)d, \quad \text{such that} \quad F_j(x_1^{(0)}, \ldots, x_N^{(0)}) = 0, \quad \text{for every } j = 1, \ldots, N. \tag{44}$$

The lattice constant $d$ depends on the choice of parameters $\zeta$ and $\mathcal{A}$ according to Eqs. (35a) and (35b), and the position $x_1^{(0)}$ is fixed by the relative phases of the pump beams. Next we add a small perturbation to this lattice, in the form of a random configurational noise. We denote the position of each cloud with respect to its equilibrium position by $\xi_j$, such that

$$x_j(t) = x_j^{(0)} + \xi_j(t), \tag{45}$$

and the initial displacement $\xi_j(t=0)$ is a uniformly distributed random variable between $-\xi_{\text{initial}}$ and $+\xi_{\text{initial}}$, with specifically $\xi_{\text{initial}}=5\times10^{-4}\lambda$. We also start the clouds with random velocities uniformly distributed between $-\omega_{\text{osc}}\xi_{\text{initial}}$ and $\omega_{\text{osc}}\xi_{\text{initial}}$.

In optical lattices with symmetric pumping (an example shown in Fig. 6), the atom clouds oscillate almost independently, and roughly with the expected time scale of $\tau_{\text{osc}}$ [as seen in Fig. 6(a)]. However, instead of centering on $\xi=0$, these oscillations are uniformly displaced, and this displacement itself varies with time in an oscillating fashion. Thus, the center-of-mass oscillations of the whole lattice have a longer time scale, in the example shown in Fig. 6, this is roughly $10\omega_{\text{osc}}$. The total intensity inside the structure is not homogeneous: the random displacements create some "cavities" where some extra light is trapped, or from where extra light can be expelled. As the atom clouds oscillate, so does the intensity, around the average value of $I_0+I_1$ roughly with

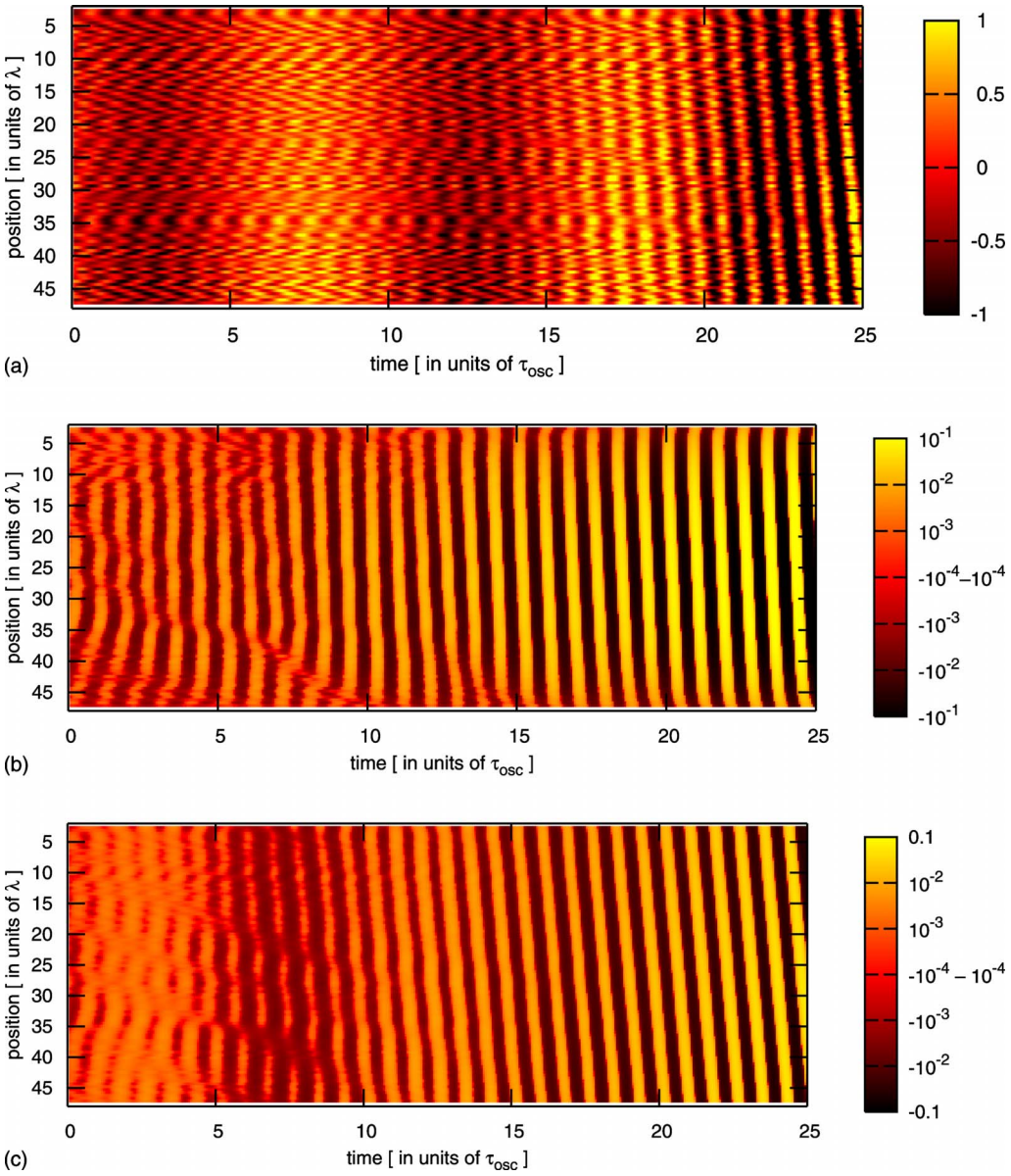


FIG. 8. (Color online) Numerical simulation of the dynamics of an optical lattice of $N=100$ clouds with polarizability $\zeta=0.1$ each, with asymmetric pumping $I_1=1.42I_0$ after initial excitation (random displacement from the equilibrium with maximum magnitude $\xi_{\text{initial}}=5\times10^{-4}\lambda$ and random velocity of maximum magnitude $\omega_{\text{osc}}\xi_{\text{initial}}$). No friction forces are assumed ($\mu=0$). Color coding stands for position distortions $\xi$ in (a), excess intensity $[I(x)-(I_0+I_1)]$ in (b), and excess pump asymmetry $[I_{\text{left}}(x)/I_{\text{right}}(x)-I_1/I_0]$ in (c).

the frequency $\omega_{\text{osc}}$. The local pump power ratio, the ratio of left–to right–propagating intensities, however, is roughly independent of position in the lattice, and oscillates at the same rate as the center-of-mass, at $\omega_{\text{osc}}$. This produces a signal—the variation of the transmitted intensities—that could be used for detection of the "slow" center-of-mass oscillations. This is the signal that would be expected for a single beam splitter oscillating at the slow frequency $10\omega_{\text{osc}}$, resulting from the change of the phases acquired by the beams until they reach the beam splitter.

Friction damps the oscillations of the atom clouds, and in the overdamped limit—an example shown in Fig. 7—as expected, instead of oscillations we only see the damping of the initial noise. The center-of-mass relaxes on a longer time scale here too, but much longer: in Fig. 7, this time scale is roughly $100\tau_d$.

This picture is drastically changed in the presence of pump asymmetry. In the example shown in Fig. 8, we set $I_1=1.42I_0$. Initially, in the first $10\tau_{\text{osc}}$, the qualitative features familiar from the symmetric pumping case can be observed, the only difference being that the local pump power ratio now depends on $x$, as seen in Fig. 8(c). Thereafter, however, the oscillations of neighboring atom clouds appear to phase lock, and thus a density wave appears in the system, propagating in the direction opposite to the stronger laser beam, crossing the whole lattice once every $\tau_{\text{osc}}$. This wave determines all of the three plotted properties, and is amplified in time. In fact, this amplification is exponential, and after

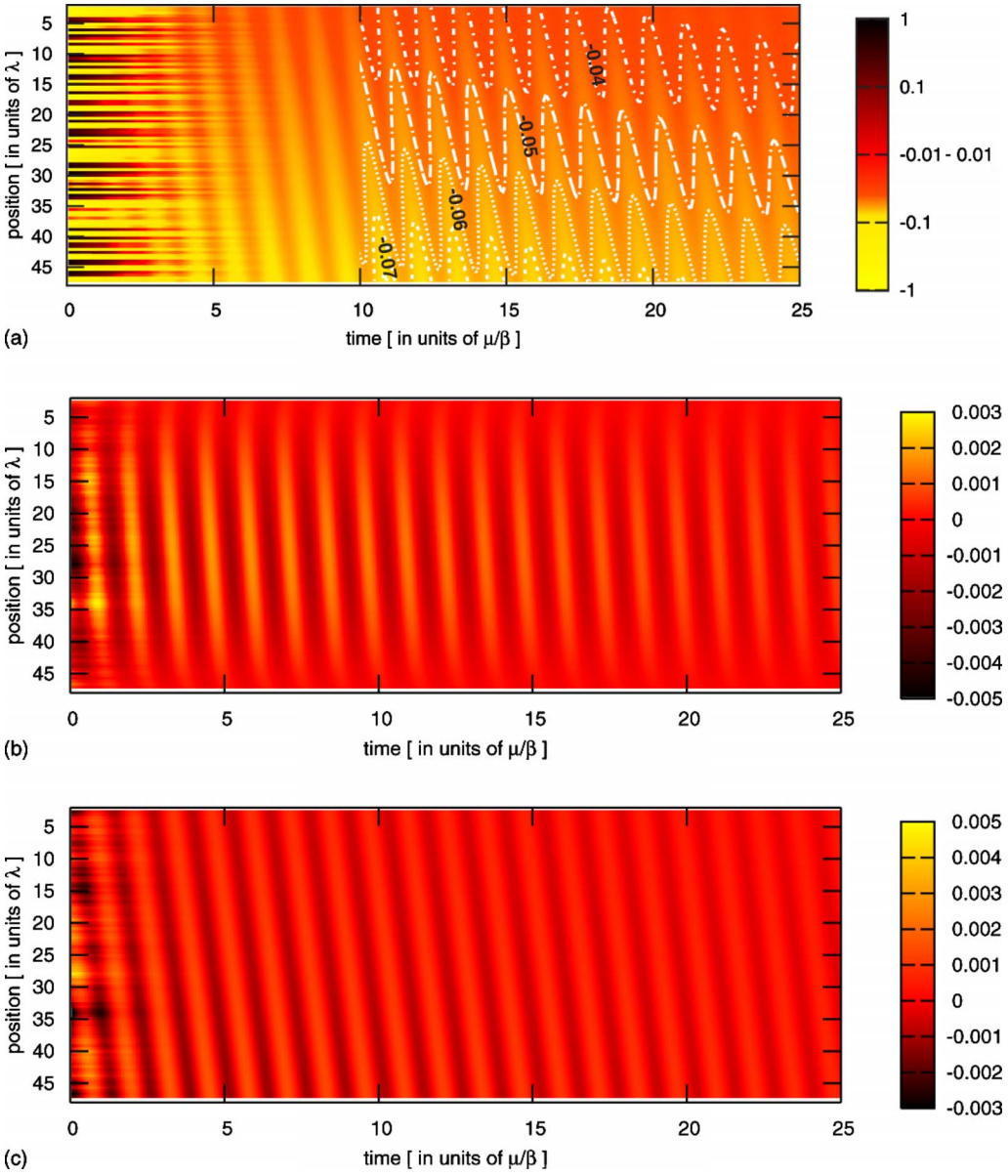


FIG. 9. (Color online) Numerical simulation of the dynamics of an optical lattice of $N=100$ clouds with polarizability $\zeta=0.1$ each, with asymmetric pumping $I_1=1.87I_0$, after initial excitation (random displacement from the equilibrium with maximum magnitude $\xi_{\text{initial}}=5\times10^{-4}\lambda$). The overdamped limit is assumed ($\mu^2 \gg \beta m$). Color coding stands for position distortions $\xi$ in (a), excess intensity $[I(x)-(I_0+I_1)]$ in (b), and excess pump asymmetry $[I_{\text{left}}(x)/I_{\text{right}}(x)-I_1/I_0]$ in (c). In (a), for better readability, for $t>10\mu/\beta$ some contour lines are shown, from top to bottom: $\xi=-0.04\xi_{\text{initial}}$ (dash-dotted), $\xi=-0.05\xi_{\text{initial}}$ (dash-dot-dotted), $\xi=-0.06\xi_{\text{initial}}$ (short dashed), and $\xi=-0.06\xi_{\text{initial}}$ (long dashed).

roughly another $10\tau_{\text{osc}}$ the amplitudes of the cloud oscillations are so large that some clouds merge, and, eventually, the whole lattice is pushed away by the stronger beam.

The overdamped limit of the dynamics in an asymmetric trap reveals even more surprises. Starting the simulation with the same realization of noise as in Fig. 7, but a larger pump asymmetry, $I_1=1.87I_0$, we observe (see Fig. 9) that most of the initial excitation is damped out as before. However, the same phase-locked oscillations as seen for the undamped case appear here, and the clouds oscillate in spite of overdamping. The amplitude of oscillations is larger for larger $x$, i.e., it increases toward the source of the stronger pump. The oscillations are all damped with the same time scale of—for these parameters—roughly $22\tau_d$, and on a longer time scale of roughly $100\tau_d$ the center-of-mass relaxes as well. Increasing the asymmetry further, to $I_1=1.88I_0$, leads to an instability very similar to that occurring in the undamped case. As seen in Fig. 10(a), after a few $\tau_d$ most of the initial excitation dies out, except for the displacement of the center-of-mass and for the density wave with wavelength equal to the system size. Now, however, this wave is amplified, and between 15 and $20\tau_d$ the dynamics of the lattice is changed. The lattice breaks into two blocks, each of them with roughly the original lattice constant $d$, the one to the left is displaced toward the right, the one to the right displaced toward the left. As shown in Fig. 11, in both slabs the average lattice

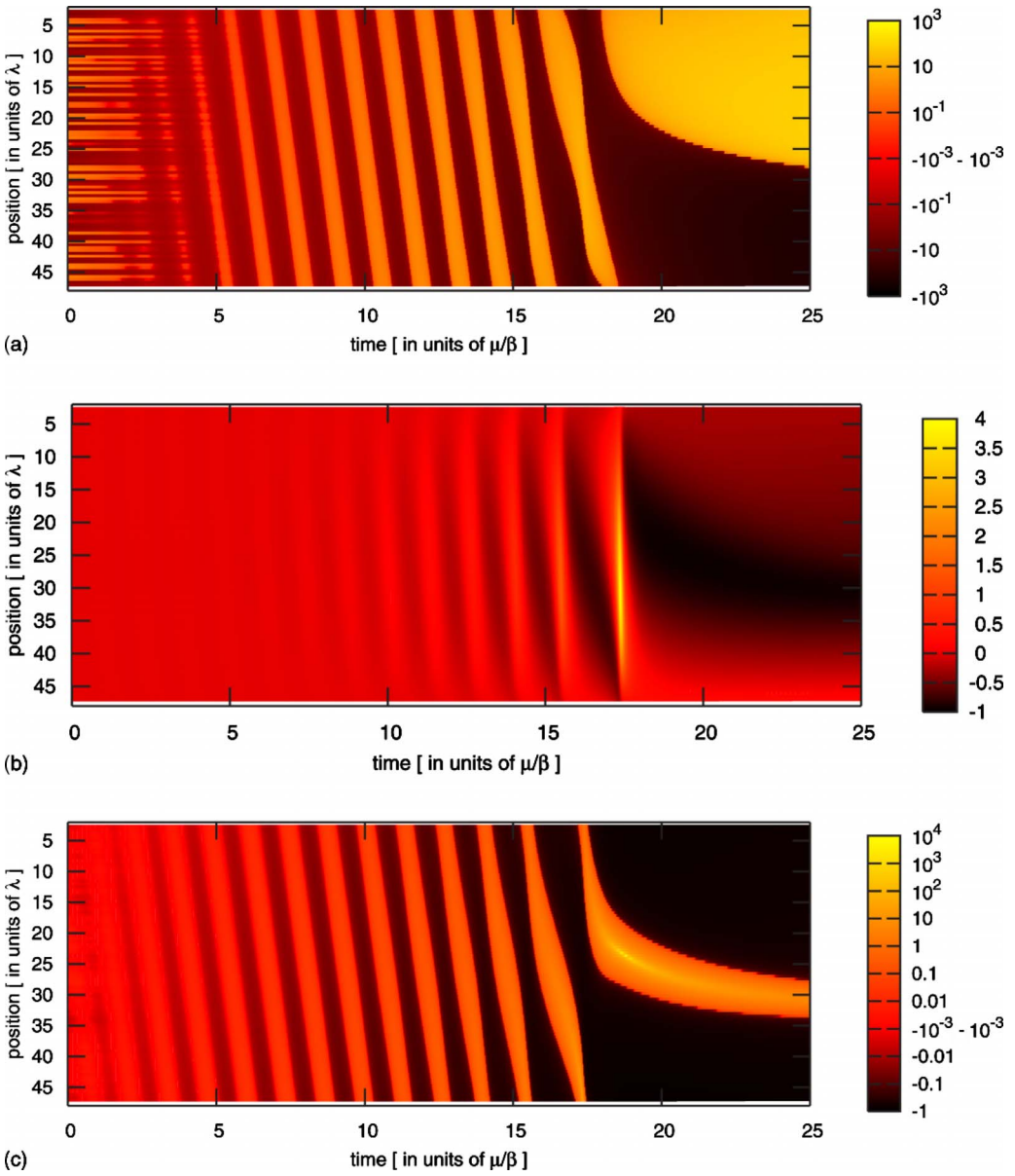


FIG. 10. (Color online) Numerical simulation of the dynamics of an optical lattice of $N=100$ clouds with polarizability $\zeta=0.1$ each, with asymmetric pumping $I_1=1.88I_0$, after initial excitation (random displacement from the equilibrium with maximum magnitude $\xi_{\text{initial}}=5\times10^{-4}\lambda$). The overdamped limit is assumed ($\mu^2 \gg \beta m$). Color coding stands for position distortions $\xi$ in (a), excess intensity $[I(x)-(I_0+I_1)]$ in (b), and excess pump asymmetry $[I_{\text{left}}(x)/I_{\text{right}}(x)-I_1/I_0]$ in (c).

constant is slightly above the expected value based on Eqs. (35a) and (35b). At their boundary, which in this run happens to be around $x=30\lambda$, the lattice constant is reduced, and, as shown in Fig. 10(b), the intensity is reduced as well. Thus optical forces push the two blocks toward each other. Later, at about $t\approx45\tau_d$, the blocks meet, and at their boundary two atom clouds merge (this is not shown in the figure). Subsequently, other clouds merge as well and eventually (after thousands of $\mu/\beta$) the whole structure will be pushed away by the stronger beam. Note that $I_1/I_0\approx1.87$ corresponds to $\mathcal{A}\approx0.64$ and therefore the Figs. 9 and 10 are both in the parameter regime denoted by the (orange) circle in Fig. 5.

After giving a taste of the dynamics in the undamped and overdamped limit, we now summarize some of the qualitative observations based on the simulations of the full equations of motion (36). For symmetric lattices, both the oscillation and the damping time scales of the center-of-mass of the structure are longer than those of the motion of the individual clouds. At small asymmetries, due to damping, the system still settles down to an equilibrium, which can be a regular optical lattice. For asymmetries exceeding a critical value $\mathcal{A}>\mathcal{A}_{\text{crit}}$, but easily satisfying $\mathcal{A}<2/\zeta$, however, the steady state optical lattice configuration is never attained. Clouds merge and, in typical runs, eventually the whole structure is pushed away by the stronger beam. Increasing the friction $\mu$ can help to stabilize the system, i.e., increase $\mathcal{A}_{\text{crit}}$. However, friction only helps up to a limit: there is a value of the asymmetry $\mathcal{A}_*$, such that if $\mathcal{A}>\mathcal{A}_*$, even the overdamped dynamics fails to converge to the optical lattice—and, typically, for this second limit we also have

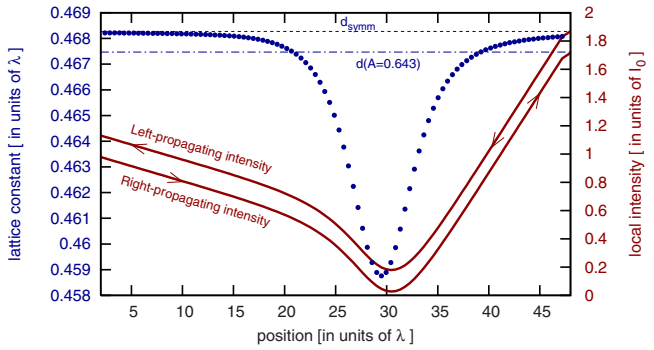


FIG. 11. (Color online) Snapshot of the simulation plotted in Fig. 10 at time $t=25\,\mu/\beta$. The local lattice constant is shown in blue points, with the lattice constant $d_{\mathrm{symm}}$ corresponding to symmetric pumping, and the equilibrium lattice constant $d$ with the asymmetry used here $\mathcal{A}=0.643$ also displayed for reference. The continuous (red) lines show the variation of the intensities in the left- and rightwards propagating modes inside the structure (their sum is the total intensity).

$\mathcal{A}_* \ll 2/\zeta$. Curiously, although oscillations die out faster and faster if the damping coefficient $\mu$ is increased, they do not disappear as $\mu \to \infty$. We have oscillations even in the overdamped limit. As intuitively expected, both $\mathcal{A}_{\mathrm{crit}}$ and $\mathcal{A}_*$ are smaller if the clouds have larger polarizability $\zeta$. Quite surprisingly, however, $\mathcal{A}_{\mathrm{crit}}$ and $\mathcal{A}_*$ depend on the number of clouds $N$ in the structure: both $\mathcal{A}_{\mathrm{crit}}(\zeta,\mu,N)$ and $\mathcal{A}_*(\zeta,N)$ decrease with increasing $N$. Thus, an asymmetric trap can only support a finite number of atom clouds with polarizability $\zeta$: even though an equilibrium optical lattice configuration with any $N$ exists, this configuration is unstable for $N > N_{\mathrm{crit}}(\zeta,\mu,\mathcal{A})$.

Due to the above listed curious effects, the asymmetry-induced contraction of the optical lattice given by Eqs. (35a) and (35b) and plotted in Fig. 5 would not occur in a real experiment with extremely asymmetric dipole trap. Even

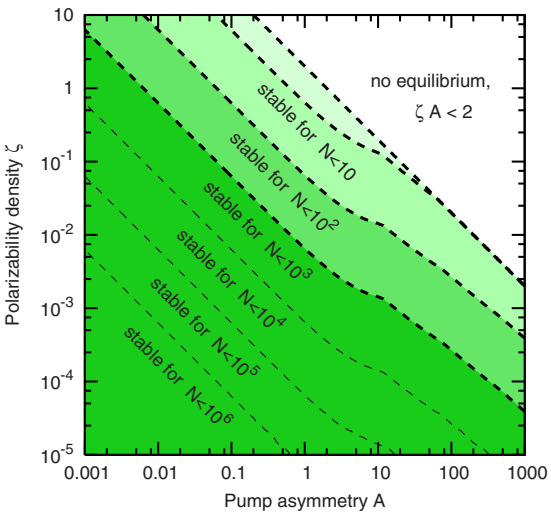


FIG. 12. (Color online) Parameter regimes where an optical lattice can be stabilized by viscous friction. White area is unstable, see Eq. (25). Thick slashed lines correspond to the slashed lines on Fig. 5

with an arbitrary amount of viscous friction, if $\mathcal{A} > \mathcal{A}_*(\zeta,N)$, the lattice would become unstable and be destroyed. This is already illustrated on Fig. 5, where the (green) shaded areas limited by dashed lines are the parameter regimes where optical lattices of specific sizes can be created (i.e., stabilized by viscous friction), for various values of $N$. The boundary between the darkest and second darkest areas [which is hardly resolved in Fig. 5(b)] corresponds to the onset of the instability for $N=1000$; the two subsequent boundaries are for $N=100$ and $N=10$. The last dashed line, the one that separates the white area from the one with the lightest shade, corresponds to $\zeta=2/\mathcal{A}$, and is in fact the limit of stability for an OL consisting of 2 clouds as well as for a single cloud. These limits of stability are also plotted directly as functions of $\zeta$ and $\mathcal{A}$ in Fig. 12, where the color coding is the same as in Fig. 5, but data for larger lattice sizes is also included [41].

## V. DYNAMICS NEAR EQUILIBRIUM: ANALYTICAL RESULTS

We can gain an analytical understanding of the phenomena listed above by studying the dynamics infinitesimally close to an equilibrium configuration. There we can develop the optical force on all of the clouds into a Taylor series, and from the nonlinear Eq. (36) we obtain, using the notations introduced in Eqs. (45) and (44), the linearized form

$$m\ddot{\xi}_j = -\mu\dot{\xi}_j + \sum_{l=1}^{N} D_{jl}\xi_l, \tag{46}$$

where the matrix $\mathbf{D}$ is defined by

$$D_{jl} = \frac{\partial}{\partial x_l} F_j(x_1 = x_1^{(0)}, \ldots, x_N = x_N^{(0)}) \tag{47}$$

or, in a more suggestive way,

$$D_{jl} = \lim_{\xi \to 0} \frac{1}{\xi} F_j(x_n = x_n^{(0)} + \delta_{ln}\xi,\ n = 1, \ldots, N). \tag{48}$$

In Eq. (46) we have a set of $N$ coupled linear differential equations. The diagonal part of $\mathbf{D}$ describes the oscillations of the clouds around their equilibrium positions. The off-diagonal terms are responsible for coupling these oscillations: they contain the interaction mediated by the trapping laser field. To understand the dynamics we need to find the eigenvectors and eigenvalues of $\mathbf{D}$. These will provide us with the noninteracting vibrational modes: their spatial structure, their frequencies and their damping coefficients. We detail the calculations below, broken down into several steps. For these calculations, for simplicity we assume purely dispersive interaction $\zeta \in \mathbb{R}$.

### A. Eigenmodes of light in the lattice

To find the force on the $j$th cloud, given by Eq. (21), we have to obtain $A_j$, $B_j$, $C_j$, and $D_j$. The first step to their calculation is to find the eigenvectors of the transfer matrix of one unit of the lattice, $\mathbf{M}(k,d)$ (see Sec. I). We fix the pump power ratio $\mathcal{P}$, which gives the lattice constant $d$ via

Eqs. (35a) and (35b), and set $k=2\pi/\lambda$, i.e., we calculate the transmission of the light constituting the periodic dipole trap. The periodicity of the optical lattice suggests that one of the eigenvectors is

$$\mathbf{u} = e^{ikd}\mathbf{P}(-d)\begin{pmatrix}\sqrt{\mathcal{P}}\\ e^{i\chi}\end{pmatrix} = \begin{pmatrix}\sqrt{\mathcal{P}}\\ e^{-i\chi}\end{pmatrix}; \quad \text{eigenvector of } \mathbf{M}, \text{ eigenvalue } e^{+i\Theta}, \tag{49}$$

where the factor $e^{ikd}$ was introduced for convenience, and we used Eqs. (35a) and (35b). We find that indeed $e^{i\Theta}\mathbf{u} = \mathbf{M}_{\mathrm{BS}}\mathbf{P}(d)\mathbf{u}$, if $\Theta=\varphi+\chi+kd$, whereby, using Eqs. (29), (35a), and (35b) we have for both red and blue detuning

$$\sin\Theta = \frac{1}{2}|\zeta|\mathcal{A}, \quad \cos\Theta = -\frac{1}{2}\sqrt{4-\zeta^2\mathcal{A}^2}. \tag{50}$$

The other eigenvector can be found using Eq. (17), the reflection symmetry of the BS: $\boldsymbol{\sigma}\mathbf{P}(d)\mathbf{u}=\mathbf{M}_{\mathrm{BS}}\boldsymbol{\sigma}e^{i\Theta}\mathbf{u} = e^{i\Theta}\mathbf{M}_{\mathrm{BS}}\mathbf{P}(d)[\mathbf{P}(-d)\boldsymbol{\sigma}\mathbf{u}]$, and by the reflection symmetry of free propagation $\boldsymbol{\sigma}\mathbf{P}(d)=\mathbf{P}(-d)\boldsymbol{\sigma}$ we have

$$\mathbf{w} = e^{-ikd}\mathbf{P}(-d)\boldsymbol{\sigma}\mathbf{u} = \begin{pmatrix}e^{i\chi}\\ \sqrt{\mathcal{P}}\end{pmatrix}; \quad \text{eigenvector of } \mathbf{M}, \text{ eigenvalue } e^{-i\Theta}, \tag{51}$$

corresponding to asymmetric pumping with $I_0>I_1$. As expected, for propagation of the trap beams we have $\Theta\in\mathbb{R}$, ensuring that these beams do indeed permeate the lattice unattenuated. Note that as $\mathbf{M}$ is not Hermitian, $\mathbf{u}$ and $\mathbf{w}$ do not form an orthonormal basis: $\mathbf{u}^\dagger\mathbf{u}=\mathbf{w}^\dagger\mathbf{w}=1+\mathcal{P}$ and $\mathbf{u}^\dagger\mathbf{w} = 2\sqrt{\mathcal{P}}e^{i\chi}$.

### B. Propagation of light in the perturbed lattice

We now compute the mode amplitudes $A_j$, $B_j$, $C_j$, $D_j$ inside an optical lattice composed of purely dispersively scattering identical clouds. At equilibrium, with $|E_1|^2=\mathcal{P}|E_0|^2$, we have an equidistant lattice with lattice constant given by Eqs. (35a) and (35b), and, as seen above,

$$\begin{pmatrix}A_j\\ B_j\end{pmatrix} = \mathbf{M}^{N-j+1}\begin{pmatrix}C_N\\ D_N\end{pmatrix} = \mathbf{M}^{N-j+1}\mathcal{E}_0\mathbf{u} = \mathcal{E}_0 e^{i(N-j+1)\Theta}\mathbf{u}, \tag{52}$$

with the complex factor $\mathcal{E}_0=E_1e^{-ik(x_N+d)}\mathcal{P}^{-1/2}$; note that $|\mathcal{E}_0| = |E_0|$.

Now if we perturb the optical lattice by displacing the $l$th element by $\xi$, as in Eq. (48), the transfer matrix of the whole structure is changed, and this affects the outgoing modes. We can then write the fields at the far left end of the structure in terms of the fields at the far right end in the following way:

$$e^{iN\Theta}\mathbf{u} + \frac{\xi}{k}\begin{pmatrix}a^{(l)}\\ 0\end{pmatrix} = \mathbf{M}^{l-1}\mathbf{P}(\xi)\mathbf{M}_{\mathrm{BS}}\mathbf{P}(-\xi)\mathbf{P}(d)\mathbf{M}^{N-l} \times\left[\mathbf{u} + \frac{\xi}{k}\begin{pmatrix}0\\ b^{(l)}\end{pmatrix}\right]. \tag{53}$$

The perturbations can be expanded in the basis given by the eigenvectors $\mathbf{u}$ and $\mathbf{w}$:

$$\begin{pmatrix}a^{(l)}\\ 0\end{pmatrix} = a_u^{(l)}\mathbf{u} + a_w^{(l)}\mathbf{w}, \quad a_u^{(l)} = -\sqrt{\mathcal{P}}e^{i\chi}a_w^{(l)},$$

$$a^{(l)} = -(\mathcal{P}-1)e^{i\chi}a_w^{(l)}, \tag{54a}$$

$$\begin{pmatrix}0\\ b\end{pmatrix} = b_u^{(l)}\mathbf{u} + b_w^{(l)}\mathbf{w}, \quad b_w^{(l)} = -\sqrt{\mathcal{P}}e^{-i\chi}b_u^{(l)},$$

$$b^{(l)} = -(\mathcal{P}-1)e^{-i\chi}b_u^{(l)}. \tag{54b}$$

Note that to first order in $\varepsilon=\xi/k$,

$$\mathbf{P}(\varepsilon/k)\mathbf{M}_{\mathrm{BS}}\mathbf{P}(-\varepsilon/k) = \mathbf{M}_{\mathrm{BS}} - 2\varepsilon\zeta\boldsymbol{\sigma}, \tag{55}$$

with the matrix $\boldsymbol{\sigma}$ corresponding to reflection about $x$ as defined in Eq. (16). We can now gather the first-order terms from Eq. (53), and have

$$a_u^{(l)}\mathbf{u} + a_w^{(l)}\mathbf{w} = \mathbf{M}^N(b_u^{(l)}\mathbf{u} + b_w^{(l)}\mathbf{w}) - 2\varepsilon\zeta\mathbf{M}^{l-1}\boldsymbol{\sigma}\mathbf{P}(d)\mathbf{M}^{N-l}\mathbf{u} = b_u^{(l)}e^{iN\Theta}\mathbf{u} + b_w^{(l)}e^{-iN\Theta}\mathbf{w} + 2|\zeta|e^{-i\chi}e^{i(N-2l+1)\Theta}\mathbf{w}. \tag{56}$$

The $\mathbf{u}$ and $\mathbf{w}$ components of this equation, together with the relations (54) give

$$a_w^{(l)} = -2|\zeta|e^{-i\chi}e^{i(2N-2l+1)\Theta}\frac{1}{\mathcal{P}e^{-iN\Theta}-e^{iN\Theta}}, \tag{57a}$$

$$b_u^{(l)} = 2|\zeta|\sqrt{\mathcal{P}}e^{i(N-2l+1)\Theta}\frac{1}{\mathcal{P}e^{-iN\Theta}-e^{iN\Theta}}. \tag{57b}$$

Note that each of these expressions contains the denominator $\mathcal{P}e^{-iN\Theta}-e^{iN\Theta}$, which can give a resonant enhancement for certain values of the asymmetry.

We can now proceed to calculate the mode amplitudes inside the perturbed optical lattice using the transfer matrices. For $j>l$, i.e., light to the right of the displaced cloud (the stronger beam is the one incident from the right), we have

$$j>l: \quad \begin{pmatrix}A_j\\ B_j\end{pmatrix} = \mathcal{E}_0\mathbf{M}^{N-j+1}[\mathbf{u} + \varepsilon b_u^{(l)}(\mathbf{u} - \sqrt{\mathcal{P}}e^{-i\chi}\mathbf{w})] = \mathcal{E}_0 e^{i(N-j+1)\Theta}\mathbf{u} + \epsilon\mathcal{E}_0 b_u^{(l)}[e^{i(N-j+1)\Theta}\mathbf{u} - e^{-i(N-j+1)\Theta}\sqrt{\mathcal{P}}e^{-i\chi}\mathbf{w}]. \tag{58}$$

To first order in $\varepsilon$ we then have

$$\frac{|A_j|^2+|B_j|^2}{|E_0|^2} = \mathcal{P}+1+2\varepsilon(\mathcal{P}+1)\mathrm{Re}\, b_u^{(l)} - 4\mathcal{P}\varepsilon\ \mathrm{Re}[b_u^{(l)}e^{-2i(N-j+1)\Theta}]. \quad (59)$$

For $j<l$, the transfer matrix of the displaced $l$th cloud also enters the calculation:

$$\begin{aligned}\begin{pmatrix}A_j\\B_j\end{pmatrix} &= \mathcal{E}_0[\mathbf{M}^{N-j+1} - 2\varepsilon\zeta\mathbf{M}^{l-j}\boldsymbol{\sigma}\mathbf{P}(d)\mathbf{M}^{N-l}]\\ &\times[\mathbf{u}+\varepsilon b_u^{(l)}(\mathbf{u}-\sqrt{\mathcal{P}}e^{-i\chi}\mathbf{w})]\\ &= \mathcal{E}_0 e^{i(N-j+1)\Theta}\mathbf{u} + \varepsilon\mathcal{E}_0[b_u^{(l)}e^{i(N-j+1)\Theta}\mathbf{u}\\ &- b_u^{(l)}e^{-i(N-j+1)\Theta}\sqrt{\mathcal{P}}e^{-i\chi}\mathbf{w} - 2\zeta e^{i(N-2l+j)\Theta}e^{ikd}\mathbf{w}].\end{aligned} \quad (60)$$

In this case, to first order in $\epsilon$ the sum of the intensities gives

$$\frac{|A_j|^2+|B_j|^2}{|E_0|^2} = \mathcal{P}+1+2\varepsilon(\mathcal{P}+1)\mathrm{Re}\, b_u^{(l)} - 4\mathcal{P}\varepsilon\ \mathrm{Re}[b_u^{(l)}e^{-2i(N-j+1)\Theta}] + 8|\zeta|\sqrt{\mathcal{P}}\varepsilon\ \mathrm{Re}\ e^{i(2j-2l-1)\Theta}. \quad (61)$$

### C. Explicit form of D

Using the above formulas (59) and (61), we can read off the forces, and obtain

$$D_{jl} = \begin{cases} 2\beta\sin\Theta\ \mathrm{Im}\dfrac{\mathcal{P}e^{2i(j-l)\Theta}}{\mathcal{P}-e^{i2N\Theta}}, & j>l,\\ -2\beta\sin\Theta\ \mathrm{Im}\dfrac{\mathcal{P}}{\mathcal{P}-e^{i2N\Theta}}+\beta\cos\Theta, & j=l,\\ -2\beta\sin\Theta\ \mathrm{Im}\dfrac{e^{2iN\Theta}e^{2i(j-l)\Theta}}{\mathcal{P}-e^{i2N\Theta}}, & j<l,\end{cases} \quad (62)$$

where $\beta$ is given by Eq. (37), and $\omega_{\mathrm{osc}}$ by Eq. (38). For symmetric pumping we can take the limit $|E_1|\to|E_0|$ of Eq. (62), and find quite simply [42]

$$D_{jl} = -\beta\delta_{jl} + \beta\frac{N\zeta^2}{1+N^2\zeta^2}. \quad (63)$$

### D. Lattice vibration eigenmodes

For symmetric pumping, close to equilibrium, substitution of Eq. (63) into Eq. (46) gives

$$F_j = -\beta\frac{1}{1+N^2\zeta^2}\xi_j + \beta\frac{N\zeta^2}{1+N^2\zeta^2}\sum_{l\neq j}(\xi_l-\xi_j). \quad (64)$$

The clouds behave as uniformly coupled oscillators. The coupling of the oscillators is independent of the distance $j-l$ of the sites, but does depend on the size $N$ of the whole structure. This coupling can be enhanced by increasing the system size $N$, however, it reaches a maximum of $\beta|\zeta|/2$ when $N|\zeta|=1$, and further increase of $N$ results in a decrease of the coupling roughly as $1/N$. It is quite clear that the coupling does not affect the common mode (or center-of-mass motion) of the lattice, i.e., when all of the clouds oscillate with the same phase. As seen from Eq. (64), the "spring constant" and the oscillation frequency, of this mode are

$$z_0 = -\beta\frac{1}{1+N^2\zeta^2}, \quad \omega_0 = \frac{\omega_{\mathrm{osc}}}{\sqrt{1+N^2\zeta^2}}. \quad (65)$$

The spring constant $z_0$ is lower in magnitude than the naive expectation of $z_{\mathrm{single}}=-\beta/(1+\zeta^2)$ from Eq. (37), whereby the oscillations of the center-of-mass are slower than naively expected. For all other modes of vibration, orthogonal to the center-of-mass mode, however, the coupling increases the frequencies. Using Eq. (63) it is directly seen that they are degenerate, and have the spring constant and oscillation frequency

$$z_1 = z_2 = \ldots = z_N = -\beta; \quad \omega_1 = \omega_2 = \ldots = \omega_N = \omega_{\mathrm{osc}} \quad (66)$$

slightly larger in magnitude than the naive expectations $z_{\mathrm{single}}$ and $\omega_{\mathrm{single}}$. For the examples plotted in Figs. 6 and 7, $N\zeta=10$ resulted in the approximately tenfold slower oscillations and 100 times slower damping of the center-of-mass, than of the other modes.

For asymmetric pumping ($|E_1|>|E_0|$), the analysis of the dynamics is considerably more involved. The main problem is that the matrix $\mathbf{D}$ itself is not symmetric any more. Thereby, the force $F_j$ is not conservative, not even in the infinitesimal neighborhood of the equilibrium configuration: If it were, $F_j=-\partial/\partial x_j V(x_1\ldots x_N)$ would imply that $\mathbf{D}$ is a Hessian matrix, symmetric by Young's theorem. We remark that asymmetric force matrices have been found in studies of the stability of the two-dimensional equilibrium configurations of optically trapped microspheres in a single plane transverse to the standing wave [28].

Although for asymmetric pumping $\mathbf{D}$ is not symmetric, we can still look for the eigenmodes of lattice vibrations, given by the eigenvectors of $\mathbf{D}$. This task is involved, since the eigenvalues and eigenvectors of a nonsymmetric real matrix can be complex, not orthogonal to each other, and are in general complicated to find. Note, however, an important symmetry of the system close to equilibrium, revealed by Eq. (62): $\mathbf{D}$ is a Toeplitz matrix (i.e., $D_{j+1,l+1}=D_{j,l}$ for every $j,l=1,\ldots,N-1$), and thus the coupling between two clouds only depends on their distance $l-j$. If $\mathbf{D}$ was a circulant matrix, i.e., it had the additional property that $D_{j,N}=D_{j+1,1}$ for every $j=1,\ldots,N-1$, its eigenvectors would be the Fourier vectors $[v_b]_j=e^{ibj2\pi/N}$, for $b=0,\ldots,N-1$. Although $\mathbf{D}$ does not have this property, a similar statement does hold for it: $D_{j,N}=\mathcal{P}D_{j+1,1}$ for every $j=1,\ldots,N-1$. Thus we can look for its eigenvectors in the following form:

$$[v_b]_j = (\mathcal{P}e^{2\pi ib})^{j/N}, \quad (67)$$

corresponding to density waves with complex wave numbers, the imaginary part the wave numbers given by $\alpha=\ln(\mathcal{P})/(Nd)$. Direct application of Eq. (62) shows that these

$\mathbf{v}_b$ are indeed eigenvectors, and after some algebra the corresponding eigenvalues $z_b$ of $\mathbf{D}$, with $b=0,\ldots,N-1$, are found to be

$$z_b = \beta \cos\Theta \left[ 1 + \frac{\zeta^2 \sqrt[N]{\mathcal{P}} \mathcal{A}^2}{(\sqrt[N]{\mathcal{P}} e^{i\pi b/N} - e^{-i\pi b/N})^2} \right]^{-1}. \quad (68)$$

This can be contrasted with the naively expected $z_{\text{single}} = \beta \cos\Theta[1+\zeta^2]^{-1}$, based on Eq. (38).

As expected, the eigenmodes (67) of the lattice vibrations are complex, except for $b=0$, which corresponds to a distorted center-of-mass mode and, if $N$ is even, $b=N/2$, the density wave of highest wave number possible $(\pi/d)$. Both of these modes are stable, as $z_{N/2} < z_0 < 0$, and damped if $\mu > 0$. Since $\mathbf{D}$ is real, all other modes form conjugate pairs: $z_b = z_{N-b}^*$ and $\mathbf{v}_b = \mathbf{v}_{N-b}^*$.

We now discuss the physical meaning of complex eigenmodes and eigenfrequencies. Consider a pair of complex eigenvalues $z_b = z_{N-b}^*$ with $0 < b < N/2$, and the corresponding eigenvectors $\mathbf{v}_b = \mathbf{v}_b^*$. Both Re $\mathbf{v}_b$ and Im $\mathbf{v}_b$ describe density waves of wave number $k_b = 2\pi b/(Nd)$, modulated so their amplitude increases exponentially with rate $\alpha = (\ln \mathcal{P})/(Nd)$ toward the source of the more intensive beam. Now since

$$\mathbf{D}\ \mathrm{Re}(\mathbf{v}_b) = \mathrm{Re}(\mathbf{D}\mathbf{v}_b) = \mathrm{Re}(z_b \mathbf{v}_b) = \mathrm{Re}\ z_b\ \mathrm{Re}\ \mathbf{v}_b - \mathrm{Im}\ z_b\ \mathrm{Im}\ \mathbf{v}_b$$

and

$$\mathbf{D}\ \mathrm{Im}(\mathbf{v}_b) = \mathrm{Im}(\mathbf{D}\mathbf{v}_b) = \mathrm{Im}(z_b \mathbf{v}_b) = \mathrm{Im}\ z_b\ \mathrm{Re}\ \mathbf{v}_b + \mathrm{Re}\ z_b\ \mathrm{Im}\ \mathbf{v}_b$$

, time evolution by Eq. (46) does not lead out of the subspace of $\mathbb{R}^N$ spanned by the modes Re $\mathbf{v}_b$ and Im $\mathbf{v}_b$. For any superposition

$$\boldsymbol{\xi}(t) = p(t)\mathrm{Re}(\mathbf{v}_b) + q(t)\mathrm{Im}(\mathbf{v}_b) = \mathrm{Re}\{[p(t) - iq(t)]\mathbf{v}_b\}, \quad (69)$$

with $p(t), q(t) \in \mathbb{R}$, Eq. (46) can be rewritten as

$$m\ddot{p} = -\mu\dot{p} + (\mathrm{Re}\ z_b)p + (\mathrm{Im}\ z_b)q, \quad (70)$$

$$m\ddot{q} = -\mu\dot{q} - (\mathrm{Im}\ z_b)p + (\mathrm{Re}\ z_b)q. \quad (71)$$

A linear combination of these two differential equations gives $m(p-iq)^{\cdot\cdot} = -\mu(p-iq)^{\cdot} + z_b(p-iq)$, a single complex homogeneous second-order linear differential equation, whose general solution can be written down straight away:

$$p(t) - iq(t) = c_+ e^{(\kappa_b^+ - i\omega_b^+)t} + c_- e^{(\kappa_b^- - i\omega_b^-)t}. \quad (72)$$

Here $c_\pm = p_\pm - iq_\pm$ are arbitrary constants and

$$(\kappa_b^\pm - i\omega_b^\pm) = \frac{-\mu \pm \sqrt{\mu^2 + 4mz_b}}{2m}, \quad (73)$$

with $\kappa_b^- < \kappa_b^+$ to fix notation, which also means $\omega_b^- < 0$ and $\omega_b^+ > 0$. Substituting the solution (72) together with Eq. (67) into Eq. (69), we have $\xi_j(t) = \xi(x=jd,t)$ for every $j = 1,\ldots,N$, with

$$\xi(x,t) = \mathrm{Re}(c_+ e^{\kappa_b^+ t} e^{\alpha x} e^{i(k_b x - \omega_b^+ t)}) + \mathrm{Re}(c_- e^{\kappa_b^- t} e^{\alpha x} e^{i(k_b x - \omega_b^- t)}). \quad (74)$$

Thus a general solution of the dynamics (infinitesimally close to equilibrium) in this subspace corresponds to two superimposed density waves of wavelength $Nd/b$, one copropagating with the stronger beam $(\omega_b^- < 0)$, and one counterpropagating $(\omega_b^+ > 0)$. Their phase velocities are given by $Nd|\omega_b^\pm|/(2\pi b)$. As $\kappa_b^- < 0$ for any values of the variables, the copropagating wave is exponentially damped with characteristic time scale $1/|\kappa_b^-|$, but the counterpropagating wave can be either damped or amplified. Thus, this pair of modes is stable if $\kappa_b^+ < 0$, which corresponds to

$$m(\mathrm{Im}\ z_b)^2 < -\mu^2\ \mathrm{Re}\ z_b. \quad (75)$$

An analogous criterion of stability has been derived for the distortions of the equilibrium patterns of optically trapped microspheres in a single plane transverse to the trap axis in Ref. [28].

For symmetric pumping $\mathcal{A}=0$, the matrix $\mathbf{D}$ is symmetric, the eigenmodes (67) are the Fourier components, and the eigenvalues (68) are all real and negative, thus the lattice is stable. As discussed a few paragraphs earlier, almost all modes have the same frequency as a single trapped cloud $z_1 = z_2 = \ldots = z_N = -\beta$ except the center-of-mass mode with $z_0 = -\beta/(1+N^2\zeta^2)$. With the introduction of a pump asymmetry $\mathcal{A} > 0$, the eigenmodes and eigenvalues (apart from $b=0$, and $b=N/2$, if $N$ is even) acquire imaginary parts, and as $\mathcal{A}$ is further increased, the real parts of the eigenvalues turn positive one by one. The first few eigenvalues are shown as functions of $\mathcal{A}$ for two examples in Fig. 13. In the "strong collective coupling" $N\zeta \gg 1$ limit [Fig. 13(a)], we observe clearly separated resonances. In this limit, whenever $\pi - \Theta \lesssim \pi/N$, we have $\sqrt[N]{\mathcal{P}} \approx 1$, and the denominator of Eq. (68) is approximately $1 - \sin^2\Theta/\sin^2(\pi b/N)$, which, with Eq. (50), places the resonance for mode $b$ at $\mathcal{A} \approx \mathcal{A}_b$, where

$$\mathcal{A}_b = b\frac{2\pi}{N\zeta}. \quad (76)$$

The simple relation $\mathcal{A} = 2\pi/(N\zeta)$ indeed fits the boundaries between the shaded green areas of Figs. 5 and 12 almost perfectly for $\mathcal{A} < 1$. Outside of the strong collective coupling regime [Fig. 13(b)], the resonances are not well resolved. It may even happen (as in the plotted example) that mode $b=2$ becomes absolutely unstable (Re $z_2 > 0$) at lower $\mathcal{A}$ than mode $b=1$. This causes the "shoulder" in the $N=10$ instability limit on Fig. 5, and on all of the slashed lines at around $\mathcal{A} \approx 10$ on Fig. 12. In Figs. 13(c) and 13(d), where the critical asymmetry is $\mathcal{A} = 2/\zeta = 20$, we have $\Theta = \pi/2$ and all eigenvalues are 0; for $\mathcal{A} > 20$ all modes are unstable. The instability rate, i.e., the largest of the $\kappa_b$, is plotted for a wider range of parameters in Fig. 14.

In the absence of damping $\mu=0$, Eq. (73) gives $\omega_b^\pm = \pm\,\mathrm{Im}\sqrt{z_b/m}$ and $\kappa_b^\pm = \pm\,\mathrm{Re}\sqrt{z_b/m}$. With asymmetric pumping the eigenvalues $z_b$ of all modes with $b \neq 0, N/2$ are complex, and thus an instability always ensues, but might be very slow on the experimental time scale (discussed in Sec. VII). As shown by Eq. (75), damping can restore the stability of

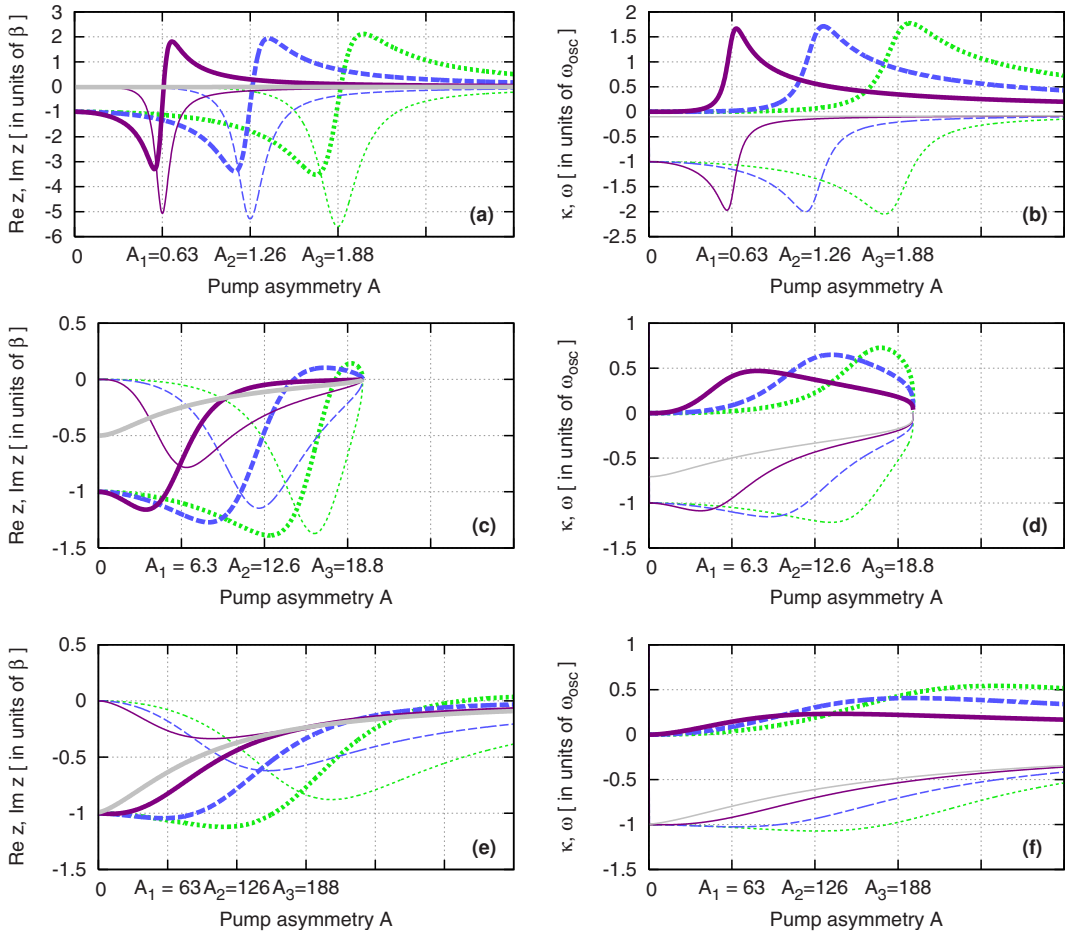


FIG. 13. (Color online) Damping rate $\kappa_b^+$ (thick) and frequency $\omega_b^+$ (thin) of the first few eigenmodes $b=0$ (continuous light gray), $b=1$ (continuous purple), $b=2$ (slashed blue), $b=3$ (dotted green) of optical lattices in the overdamped (left column) and undamped (right column) limit. In the overdamped case, these are directly given by the real and imaginary parts of the eigenvalues of the force matrix $\mathbf{D}$: $\kappa_b^+\tau_d=\mathrm{Re}\, z_b/\beta$ and $\omega_b^+\tau_d=\mathrm{Im}\, z_b/\beta$, whereas in the undamped case, by the square root of $z_b$: $\kappa_b^+/\omega_{osc}=\mathrm{Re}\sqrt{z_b/\beta}$ and $\omega_b^+/\omega_{osc}=\mathrm{Im}\sqrt{z_b/\beta}$. In (a) and (b), a lattice of $N=100$ clouds of polarizability $\zeta=0.1$ is taken, the same choice of parameters as used for the illustrations of the dynamics in Figs. 6–10. As $N\zeta=10$, this is in the strong collective coupling regime, clearly separated resonances are seen at the predicted positions. In (c) and (d), $N=10$ and $\zeta=0.1$, and thus the collective coupling is weaker, the resonances overlap strongly. As $\mathcal{A}$ approaches $2/\zeta=20$, the trap depth decreases sharply, and for $\mathcal{A}>20$ the curves do not continue as the dipole force is no longer able to hold the clouds against the scattering force. In (e) and (f), $N=1000$, and $\zeta=10^{-4}$ means that the collective coupling is weak, $N\zeta\ll 1$. Although the resonances can still be distinguished, they overlap almost completely, and the instability rate $\kappa$, the maximum of the $\kappa_b$, is a smoothly increasing function of the asymmetry.

the modes as long as the real parts of the eigenvalues are negative. The $b$th mode is overdamped if $\mu^2 \gg |z_b| m$, its dynamics is then effectively first-order (cf. Sec. IV), and the copropagating mode disappears (is damped out on a very short time scale). For the counterpropagating mode we then have $\omega_b^+=-\mathrm{Im}\, z_b/\mu$, and $\kappa_b^+=\mathrm{Re}\, z_b/\mu$. Even with arbitrarily strong damping, the OL becomes unstable if $\mathrm{Re}\, z_b>0$, as then $\kappa_b^+>0$ [and the right-hand side of Eq. (75) is negative]. This "absolute instability" is used to define the shaded areas in Figs. 5 and 12. The overdamped dynamics close to this absolute instability limit is illustrated in Figs. 9 and 10, which show the results of numerical integration of Eq. (41) near this limit.

## VI. STABILITY WITH RESPECT TO NOISE

For the simulation reported in Sec. IV as well as for the analytical calculations we considered a perfectly regular lattice made of purely dispersive and infinitely thin clouds with deterministic dynamics. However, the phenomena we found are fairly robust: these approximations can be somewhat relaxed without altering the qualitative picture. We do not go into the details very much here but illustrate this statement with examples from "noisy" simulations in Fig. 15. We simulate clouds of finite thickness by placing many (on average 10) infinitely thin sheets at a single site, the only interaction between them being that mediated by the trap light. To simulate the density inhomogeneity of an optical lattice, the sheets are distributed randomly (Poissonian distribution), in a way as to model a parabolic external confinement: $p(x) \propto \exp\{[x-20\lambda]^2/[2\times(15\lambda)^2]\}$. 1000 sheets of $\zeta=0.01+2i \times 10^{-5}$ are distributed this way over 100 lattice sites, and so an optical lattice of roughly 30 sites with $\zeta\approx 0.3+6\times 10^{-4}i$ is formed, the polarizability decreasing smoothly toward the edges. Furthermore, Dirac-$\delta$ correlated noise terms are added

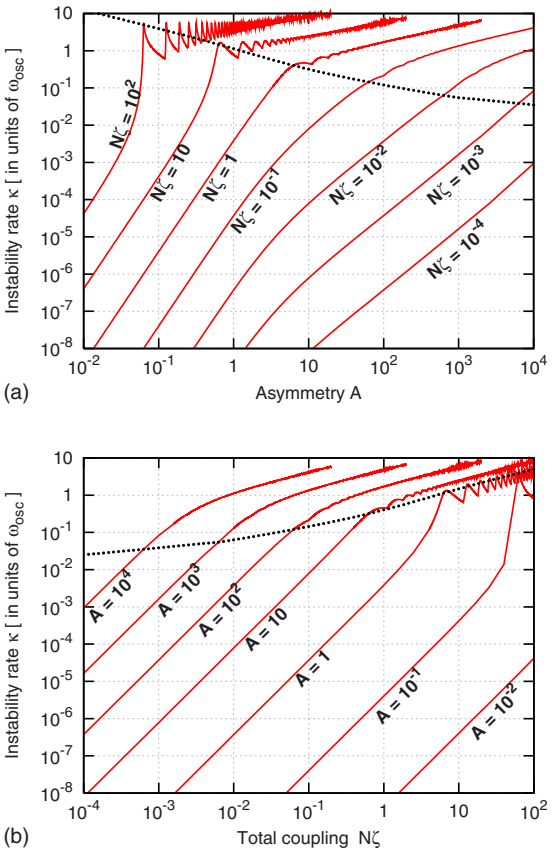


FIG. 14. (Color online) Exponential rate $\kappa$ of instability (the largest of the $\kappa_b$) for an undamped optical lattice, for various settings of the collective coupling as a function of the asymmetry (a), and for various settings of the asymmetry $\mathcal{A}$ as functions of the collective coupling $N\zeta$ (b). For these plots we set $N=1000$, but for $N \gg 1$, a change in $N$ does not affect the curves except for the termination point of the lines (which is at $\zeta\mathcal{A}=2$). Note that $\omega_{\rm osc}$ itself depends on both the asymmetry $\mathcal{A}$ and the coupling constant $\zeta$ (but not on the total number of occupied sites $N$) in a nontrivial way. On both plots, the dotted line shows the growth rate if the asymmetry is set near the first resonance, i.e., $\mathcal{A}=2\pi/(N\zeta)$. The ripples on the plots at large instability rates $\kappa>1$ are caused by the resonances illustrated in Fig. 13. For low instability rates $\kappa<0.1$, and weak total coupling $N\zeta<1$, we find that for $\kappa$ varies smoothly with $N\zeta$ and $\mathcal{A}$. Under these conditions at low asymmetries $\mathcal{A}<1$, $\kappa \approx \omega_{\rm osc}(N\zeta)^2\mathcal{A}^3/(2\pi)^3$ (analytical estimate), whereas for large asymmetries $\mathcal{A}>10$, the data can be well fitted with $\kappa \approx 0.015\omega_{\rm osc}(N\zeta)^2\mathcal{A}^{1.7}$.

to the equations of motion, which, using the reduced units [length in λ, time in $\tau_{\rm osc}$ (39), electric field in $E_0$], read

$$\dot{x}_j(t+\Delta t) = \dot{x}_j(t) + f_{CU}\frac{\eta_1}{\eta_j}(|A_j|^2 + |B_j|^2 - |C_j|^2 - |D_j|^2) - \mu_{CU}\dot{x}_j(t)\mathcal{D}\sqrt{\Delta t}\Xi, \tag{77}$$

with dimensionless constants $f_{CU}=\pi/[4|\mathrm{Re}\ \zeta_1|\sqrt{\mathcal{P}}]$, $\mu_{CU}=\mu_A[\pi\eta_1\lambda c]^{1/2}/[4m_A|\mathrm{Re}\ \zeta_1|\sqrt{\mathcal{P}I_0}]^{1/2}$, and a choice of $D_0=0.01$, where $\Xi$ is a random noise variable of average zero and variance of 1. Similarly, in the overdamped limit, where

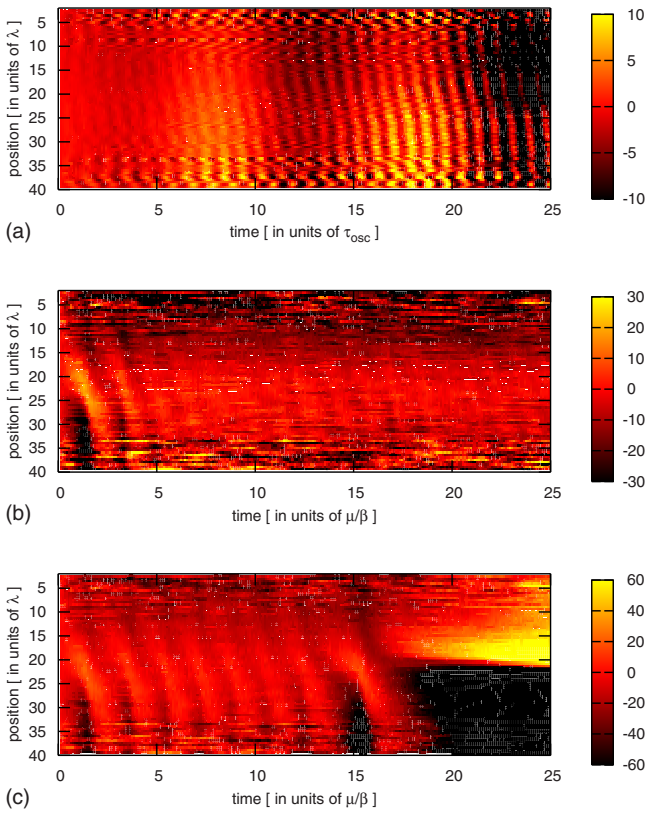


FIG. 15. (Color online) Numerical simulation of the dynamics of an optical lattice with noise. 1000 sheets of $\zeta=0.01$ are distributed over 100 lattice sites according to a Gaussian centered on $x=20\lambda$ of width 15λ. Thus $\zeta \approx 0.3$ in the center of the structure, and decreases to $\zeta \approx 0$ near the edges, with a Poissonian distribution of $\zeta$. At each site, Im $\zeta=2\times10^{-3}$ Re $\zeta$. Color coding stands for the average displacement $\xi$ of the sheets at each site is after initial excitation (random independent displacement of each sheet from equilibrium with maximum magnitude $\xi_{\rm initial}=5\times10^{-4}\lambda$ and random velocity of maximum magnitude $\omega_{\rm osc}\xi_{\rm initial}$). In (a), no friction forces are assumed ($\mu=0$), and $I_1=1.39I_0$. In (b) and (c) the overdamped limit is taken, with $I_1=1.902I_0$ and $I_1=1.904I_0$ respectively.

the time unit is $\tau_{\rm d}$ of Eq. (42), we add the noise terms to obtain

$$x_j(t+\Delta t) = x_j(t) + f'_{CU}\frac{\eta_1}{\eta_j}(|A_j|^2 + |B_j|^2 - |C_j|^2 - |D_j|^2) + \mathcal{D}\sqrt{\Delta t}\Xi, \tag{78}$$

where now $f'_{CU}=[16\pi|\mathrm{Re}\ \zeta_1|\sqrt{\mathcal{P}}]^{-1}$ and $D_0=0.01$ as above.

As seen in Fig. 15, in the regime of large collective coupling $\Sigma_j\zeta_j=10$ the same qualitative features as observed on Figs. 8–10 appear. In the undamped case (a), the center-of-mass oscillations are 10 times slower, and the other oscillations synchronize so that a density wave propagating toward the source of the stronger laser beam arises, which crosses the whole system in $\tau_{\rm osc}$. In the overdamped case, we also find the same qualitative feature of synchronization of the oscillations, and a sharp instability limit, although this occurs at slightly higher pump asymmetry, and the propagation of the wave is slower, than in the noiseless case (oscillation

time scale is roughly $2\tau_d$). Due to the inhomogeneous density distribution the shape of the propagating density wave is altered, but is still quite smooth as the long-range interaction averages out the local noise.

## VII. EXPERIMENTAL ISSUES

### A. Cold atoms

For optical lattices consisting of ultracold atoms trapped in vacuum it is cumbersome to produce viscous friction forces. In the absence of friction our model predicts that any asymmetry in the intensities of the trap beams should give rise to a dynamic instability of the lattice. However, observation of this instability can be hampered by noise. Even if all experimental precautions are made, one source of noise cannot be canceled: absorption and spontaneous emission of photons from the trapping lasers by the atoms. In the following, we discuss what experimental parameters are necessary for the dynamic instability to be substantially faster than the heating due to absorption.

Most optical lattice experiments use alkali atoms, since they have simple electronic level structure, with the trap lasers tuned near the $D$ line. We use the notation of Ref. [32], the fields are assumed to be polarized along $z$, the quantization axis for the atoms. The dipole transition matrix element $d_{eg}$ is related to the linewidth $\Gamma$ and frequency $\omega_0$ by

$$\Gamma = \frac{\omega_0^3}{3\pi\epsilon_0\hbar c^3} d_{eg}^2. \tag{79}$$

The Rabi frequency $\Omega$ gives the characteristic energy of the dipole coupling

$$\hbar\Omega(\mathbf{r}) = -d_{eg}|E(\mathbf{r})|. \tag{80}$$

Note that the value of the Rabi frequency depends on the position $\mathbf{r}$ of the atom. For red detuning, atoms will be near antinodes, and we can take $|E(\mathbf{r})| \approx |E_1| + |E_0|$. For blue detuning, cold atoms will initially be near the nodes $|E(\mathbf{r})| \approx ||E_1| - |E_0||$, however, if they are heated, the latter expression underestimates the electric field, for atoms with high kinetic energies $|E(\mathbf{r})| \approx |E_1| + |E_0|$ is more appropriate. Linear polarizability is only a good approximation if the atomic transition is not saturated. This can be ensured by choosing $|\Delta| \gg |\Omega|$: the upper-state population $\sigma_{ee}$ then reads

$$\sigma_{ee} = \frac{\Omega^2/4}{\Delta^2 + (\Gamma/2)^2} \approx \frac{\Gamma/2}{|\Delta|} \frac{3\lambda^2(I_0 + I_1)}{4\pi\hbar|\Delta|\omega} Q, \tag{81}$$

where the $Q$ is a dimensionless correction factor accounting for the effects of localization in the asymmetric trap

$$\text{red detuning:} \quad Q = 1 + \frac{2\sqrt{\mathcal{P}}}{\mathcal{P}+1}, \tag{82a}$$

$$\text{blue detuning, well trapped atoms:} \quad Q = 1 - \frac{2\sqrt{\mathcal{P}}}{\mathcal{P}+1}, \tag{82b}$$

$$\text{not well trapped atoms:} \quad Q = 1. \tag{82c}$$

We require $\sigma_{ee} < 10^{-2}$, say. In the large detuning ($|\Delta| \gg \Gamma$) and low saturation ($|\Omega| \ll |\Delta|$) limit the complex polarizability $\alpha$ of a single atom can be expressed as

$$\alpha = -\frac{d_{eg}^2}{\hbar}\frac{1}{\Delta}\left(1 + i\frac{\Gamma/2}{(-\Delta)}\right) = \frac{\Gamma/2}{(-\Delta)}\frac{3}{4\pi^2}\epsilon_0\lambda^3\left(1 + i\frac{\Gamma/2}{(-\Delta)}\right). \tag{83}$$

Thus the polarizability (divided by the transverse area) of an atom cloud reads simply

$$\zeta = \frac{k\eta\alpha}{2\epsilon_0} = \frac{\Gamma/2}{(-\Delta)}\frac{3N_\lambda}{4\pi}\left(1 + i\frac{\Gamma/2}{(-\Delta)}\right). \tag{84}$$

By virtue of Eq. (84), the back-action of the atom clouds on the field, i.e., $\zeta$, can be enhanced by working at only moderately large detuning (as opposed to the $\Delta \approx -10^7\Gamma$ of many optical lattice experiments).

The trap depth $U_{\text{dip}}$ of the dipole trap, for single atoms moving independently, can be estimated by neglecting any feedback effects on the field. The trap then has a $U(x) \propto \cos^2 kx$ form, with the trap depth given by

$$U_{\text{dip}} = \frac{1}{4}|\alpha|[(|E_0| + |E_1|)^2 - (|E_0| - |E_1|)^2]$$

$$= |\alpha E_0 E_1| = 2\hbar|\Delta|\sigma_{ee}\frac{2\sqrt{\mathcal{P}}}{Q(\mathcal{P}+1)}. \tag{85}$$

The trapped atoms absorb part of the trapping laser beams, and most of this absorbed power is reemitted as radiation with frequency close to $\omega$, corresponding to spontaneous emission, but some of it heats the motion of the atom. On average, each absorbed and spontaneously emitted photon increases the kinetic energy of the atom by an amount known as the recoil energy

$$E_{\text{rec}} = k_B T_{\text{rec}} = \frac{\hbar^2 k^2}{m_A}. \tag{86}$$

Since the rate of spontaneous emission of photons is $dN/dt = \Gamma\sigma_{ee}$, the heating rate, or the rate of increase of kinetic energy of the atoms, can be expressed as

$$P_{\text{heat}} = \Gamma\sigma_{ee}E_{\text{rec}} = \Gamma\sigma_{ee}\frac{\hbar^2 k^2}{m_A}. \tag{87}$$

Heating due to absorption leads first to a breakdown of the Dirac-$\delta$ approximation used in our model (5), and, more crucially, on a longer time scale of $t_{\text{heat}}$, the atoms eventually "evaporate" from the optical lattice. We can estimate the time scale for heating of the atoms out from the trap by

$$t_{\text{heat}} = \frac{U_{\text{dip}}}{P_{\text{heat}}} = \frac{1}{\omega}\frac{|\Delta|}{\Gamma/2}\frac{m_A c^2}{\hbar\omega}\frac{2\sqrt{\mathcal{P}}}{Q(\mathcal{P}+1)}. \tag{88}$$

For $^{87}$Rb and $^{23}$Na, this is roughly $t_{\text{heat}} \approx 10^{-5}|\Delta|/(\Gamma/2)$ s and $t_{\text{heat}} \approx 1.6 \times 10^{-6}|\Delta|/(\Gamma/2)$ s, respectively.

The back-action-induced dynamic instabilities can only be observed in an experiment if they are much faster than the evaporation

TABLE I. Some experimental requirements and the relevant time scales for the instability, for an optical lattice of $N=500$ disk-shaped clouds of areal density $\eta=10/\lambda^2$ each (corresponding to a 3D lattice with filling factor of 2.5). The pump asymmetry is set at $\mathcal{P}=10$, and laser power is chosen so that the population of the upper level is $\sigma=10^{-3}$.

| | $^{87}$Rb | | $^{23}$Na | |
|---|---|---|---|---|
| $\Delta/(\Gamma/2)$ | $-10^4$ | $-10^5$ | $-10^4$ | $-10^5$ |
| $I_0+I_1$ | 0.21 kW/cm$^2$ | 21 kW/cm$^2$ | 0.79 kW/cm$^2$ | 79 kW/cm$^2$ |
| $\zeta$ | $2.39\times10^{-4}$ | $2.39\times10^{-5}$ | $2.39\times10^{-4}$ | $2.39\times10^{-5}$ |
| $t_{\mathrm{heat}}$ | 77 ms | 770 ms | 11 ms | 116 ms |
| $\tau_{\mathrm{osc}}$ | 1.73 $\mu$s | 0.547 $\mu$s | 0.53 $\mu$s | 0.17 $\mu$s |
| $t_{\mathrm{inst}}=\kappa^{-1}$ | 0.33 ms | 10 ms | 0.10 ms | 3.2 ms |

$$\kappa t_{\mathrm{heat}} \gg 1. \tag{89}$$

As seen from Eqs. (37), (68), and (73) both $\kappa_b^{\pm}$ and $\omega_b^{\pm}$ are proportional to the oscillation frequency $\omega_{\mathrm{osc}}$ of a single atom cloud (which is the same as the oscillation frequency of a single atom) in the trap is, which is

$$\omega_{\mathrm{osc}} = \sqrt{\frac{8k|\zeta|}{c\eta m_A}}\sqrt[4]{I_0 I_1} = \sqrt{\frac{2U_{\mathrm{dip}}k^2}{m_A}} = \sqrt{\frac{2\hbar\Gamma}{m_A c^2}}\sqrt{\frac{|\Delta|}{\Gamma/2}}\sqrt{\sigma_{ee}}\omega\sqrt{\frac{2\sqrt{\mathcal{P}}}{Q(\mathcal{P}+1)}}. \tag{90}$$

As shown in Fig. 14, the constant of proportionality depends sensitively on the choice of asymmetry. Using the estimates of the caption of Fig. 14, we find that the instability is faster than dipole heating at low asymmetries $\mathcal{A}<1$ if

$$1 \ll \kappa t_{\mathrm{heat}} = 0.008\sqrt{\sigma_{ee}}\sqrt{\frac{\Gamma/2}{|\Delta|}}N^2\left(\frac{3N_\lambda}{4\pi}\right)^2\sqrt{\frac{\Gamma/2}{\omega}}\sqrt{\frac{m_A c^2}{\hbar\omega}}Q^{-3/2}\mathcal{A}^3, \tag{91}$$

whereas for large asymmetries $\mathcal{A}>10$ we have

$$1 \ll \kappa t_{\mathrm{heat}} = 0.085\sqrt{\sigma_{ee}}\sqrt{\frac{\Gamma/2}{|\Delta|}}N^2\left(\frac{3N_\lambda}{4\pi}\right)^2\sqrt{\frac{\Gamma/2}{\omega}}\sqrt{\frac{m_A c^2}{\hbar\omega}}\mathcal{A}^{-1.3}. \tag{92}$$

Roughly for $^{87}$Rb, $\omega_{\mathrm{osc}}t_{\mathrm{heat}}\approx 0.14[|\Delta|/(\Gamma/2)]^{3/2}$, whereas for $^{23}$Na, $\omega_{\mathrm{osc}}t_{\mathrm{heat}}\approx 0.070[|\Delta|/(\Gamma/2)]^{3/2}$. Some concrete examples are given in Table I.

### B. Plastic beads

Although the largest optical lattices to date consist of trapped atoms, optical forces can be used to trap much bigger objects as well. Since the earliest days of optical trapping [40] a large amount of work has gone into trapping plastic microspheres (or "beads") of diameter comparable to, or even larger than, the wavelength of the trap laser. It has been realized as early as 1989 [25], that the interference between the incident and the scattered fields gives rise to an effective interaction between microscopic beads, which later has been shown to modify the structure of one-dimensional arrays of trapped beads significantly [26,27,34]. Recently, research has focused on the transverse motion of particles which are in the same plane, trapped at an antinode of the standing-wave interference pattern of two opposing laser beams; note that this is the degree of freedom averaged out in our model. It has been found in Ref. [28] that the beads can "crystallize" into intricate periodic or quasiperiodic structures, and with the addition of new beads some modes of motion of these structures can become unstable.

In most experiments with trapped microspheres, the size of the beads is of the same order of magnitude as the wavelength of the lasers. It is usually assumed that much smaller beads, which are Rayleigh scatterers, do not have interesting dynamics [28]. However, the type of instability explored in this article could be studied with optically trapped beads of very small size instead of cold atoms. The radius of the beads should be small enough so that they can be taken as pointlike scatterers. Such experiments could be hard to perform as stronger Brownian motion makes trapping of very small beads more difficult. However, due to the overdamped dynamics of these beads, the experimental signatures of optomechanical coupling would be more straightforward to detect.

## VIII. CONCLUSIONS

We have considered the dynamics of a one-dimensional optical lattice due to the nonlinearities caused by multiple reflections of photons within the lattice. We adopted the simple model where the trap beams are approximated as plane waves, and all transverse dynamics is neglected [12]. Here the atom clouds affect the fields as beam splitters with dimensionless coupling constant $\zeta=-i\tau/t$. We supplemented this model by a derivation of the force on the trapped atom clouds, based on the Maxwell stress tensor. We have shown the corrections this force brings to the standard "radiation pressure" and "dipole force." These corrections are substantial in the regime of strong coupling (dense atom clouds, $\zeta>1$), and impose a limit on the asymmetry between the trap beam intensities even for purely dispersive atom-light interaction. We then analyzed the dynamics of large lattices, including the mechanical interaction between the trapped atom

clouds that is mediated by the trap light. Since the system is one dimensional, the interaction does not decay with the distance of the atom clouds, and thus alters the dynamics more and more substantially as the system size (number $N$ of clouds) is increased. For symmetric pumping, this leads to a softening of the center-of-mass oscillations, and a slight identical shift of all other modes of oscillation. For asymmetric pumping, it gives rise to an instability of the lattice which has the form of a density wave copropagating with the weaker beam. In the limit of strong collective coupling ($N\zeta \gg 1$) the propagation velocity and growth rate of these waves can be resonantly enhanced at certain values of the pump asymmetry $\mathcal{A}$. Although viscous friction can restore the stability of the optical lattice, there is a critical asymmetry (depending nontrivially on both $N$ and $\zeta$), above which the density waves arise and eventually destroy the lattice even in the overdamped limit.

The interaction due to multiple scattering is important for microscopic particles, trapped by light, whose size is comparable to the wavelength. In such systems effects similar to those we describe here (nonconservative forces, oscillating and unstable modes even in the overdamped limit) have already been predicted for the two-dimensional motion of "photonic clusters" in a plane transverse to the trap beams [28]. There, however, the situation is much more complex due to the higher dimensionality and to the more complicated scattering. In the Mie regime, multiple reflections within a single bead lead to nontrivial modifications with respect to the pointlike (Rayleigh) scatterer, and this is thought to be essential: in Ref. [28], it is stated that vibration frequencies of photonic clusters of Rayleigh particles are always real.

In the one-dimensional OL studied in this paper, the asymmetric pumping drives a net energy and momentum flow through the system, relating it to crystals driven far from equilibrium. Indeed, traveling density waves have been predicted to arise in arrays of vortices in a type-II superconductor [43], and have been experimentally observed and analyzed in a chain of water drops dragged by oil [44,45]. These systems, and the one we study in this Article, share the common trait that the interaction between the components (arising from the Lorentz force in the first case, and from the hydrodynamic interaction in the second) is not symmetric in the sense of Newton's third law. However, for the vortices and the water droplets, this interaction has finite range, and therefore leads to a well-defined dispersion relation in the thermodynamic limit. In our one-dimensional system, however, as the interaction is infinite range, the thermodynamic limit does not make sense. Thus there is no dispersion relation and we cannot speak of "phonons."

In this paper we have revealed that tuning the pump asymmetry opens the possibilities of using optical lattices as a model system for driven crystals far from equilibrium, a largely uncharted topic of physics. Although some of the intriguing features of the dynamics, in particular, the resonant enhancement of the instability, are specific to the optical lattice, some of them are generic (traveling density waves, complex wave vectors, etc.). This shows a way, based on optomechanical coupling, of using optical lattices to explore a subject traditionally belonging to condensed matter physics.

## ACKNOWLEDGMENTS

We acknowledge funding from the Austrian Science Foundation (Contract Nos. P17709 and S1512) and from the National Scientific Fund of Hungary (Grant Nos. NF68736 and T049234).

## APPENDIX A: THE FORCE ON AN ATOM CLOUD: DERIVATION BASED ON MULTIPLE SCATTERING

In Sec. II we have derived the optical force on an atom cloud in an asymmetric dipole trap. We have shown that to first order in the polarizability $\zeta$ of the cloud, the force can be explained in terms of the standard theory of the mechanical effects of light on atoms: it is the sum of the "radiation pressure" and the "dipole force" on each particle due the incident fields. However, the force depends nonlinearly on the polarizability $\zeta$. Inasmuch as this nonlinearity is due to the large polarizability of the individual particles, our formula (22) provides an extension of the standard formulas for the optical forces. If, however, the polarizability of each particle is small, the force on the atom cloud can be derived from the standard optical force. We provide this derivation below.

According to the standard theory of optical forces on atoms [32], in the regime of linear polarizability the force an atom in a superposition of two counterpropagating standing waves $E(x)=He^{ikx}+Ge^{-ikx}$ reads

$$\mathcal{F}=\frac{k}{2}(|H|^2-|G|^2)\mathrm{Im}\ \alpha-k\ \mathrm{Im}\ GH^*\ \mathrm{Re}\ \alpha, \tag{A1}$$

$$=-\frac{k}{2}\mathrm{Re}\{[2(\mathrm{Im}\ GH^*)+i(|H|^2-|G|^2)]\alpha\}. \tag{A2}$$

Here we have united the first term, the "radiation pressure," and the second term, the "dipole force," in a complex quantity. We would like to use this formula to find the total force on a pancake-shaped thin atom cloud, with width $l \ll \lambda$, transverse area $w \gg \lambda^2$, and total polarizability $\zeta$, in a trap with electric field incident from the left, $Be^{ikx}$, and from the right, $Ce^{-ik(x-l)}$. For $\zeta \ll 1$, the back-action of the atoms on the light field can be neglected in a zeroth approximation, and the formula (A1) can be applied directly. This is equivalent to calculating the optical force based on the Maxwell stress tensor and taking into account the modification of the light field due to the cloud only to first order in $\zeta$. For $\zeta$ of the order of 1 (or for very asymmetric pumping and $\mathrm{Im}\ \zeta < \zeta^2$), this approach constitutes a bad approximation: we need to go on.

To proceed, we divide the atom cloud into a sequence of slices such that the polarizability of each size is infinitesimal,

$$\zeta=\sum_{i=1}^{n} d\zeta_j, \quad \text{with} \quad |d\zeta_j| \ll 1 \quad \text{for every } j=1,\ldots,n. \tag{A3}$$

This is illustrated in Fig. 16. Since the whole cloud is assumed to be much thinner than $\lambda$, we neglect the phases

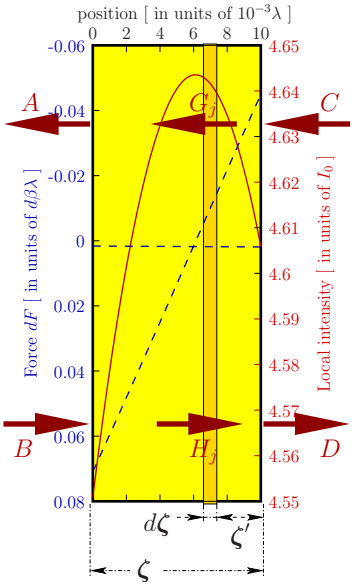


FIG. 16. (Color online) A single atom cloud, with $\zeta=0.5+0.025i$, and a slice (dark background). The intensity of the electric field (continuous red line) varies inside the atom cloud, and so does the "radiation pressure" (dotted blue line) and "dipole force" (slashed blue line), the first and second terms of the force (A1) on a single slice. The forces are plotted in units of $\lambda d\beta = 8\pi\epsilon_0 \mathrm{Re}\, d\zeta|BC|$, where $n=200$ slices were taken with coupling constant $d\zeta_1=d\zeta_2=\cdots=d\zeta_{200}=d\zeta=\zeta/200$. The dipole trap is asymmetric, with $|C|=1.5|B|$.

picked up be the light during propagation between the slices. As shown in Sec. I, for such infinitesimally closely spaced beam splitters the polarizability parameter $\zeta$ is additive, hence the requirement (A3). Now each slice only effects the electric field perturbatively ($|\mathfrak{r}_j|=|d\zeta_j|/|1-id\zeta_j|\ll 1$), and thus the field at the $j$th slice is to a good approximation the superposition of just two plane waves $E(x-x_j)=G_j e^{ik(x-x_j)}+H_j e^{-ik(x-x_j)}$, with $x_j$ denoting the position of the slice. We can find the amplitudes $G_j$ and $H_j$ simply using the additivity of $\zeta$:

$$\begin{pmatrix} H_j \\ G_j \end{pmatrix} = \begin{pmatrix} (1+i\zeta') & i\zeta' \\ -i\zeta' & (1-i\zeta') \end{pmatrix} \begin{pmatrix} C \\ D \end{pmatrix}, \quad \text{with} \quad \zeta' = \sum_{l=j+1}^{n} d\zeta_l. \tag{A4}$$

Multiplying this force by the areal atom density of the $j$th slice, $\eta_j=(d\zeta_j/\zeta)(N_\lambda/\lambda^2)$, we obtain the areal density of the force on the $j$th slice:

$$dF_j = -\epsilon_0 \,\mathrm{Re}\{[2(\mathrm{Im}\, G_j H_j^*) + i(|H_j|^2 - |G_j|^2)]d\zeta_j\}. \tag{A5}$$

The force on the whole cloud is the sum of the forces on the individual slices, which in the limit of infinitesimal slices becomes a complex integral

$$F = \sum_j dF_j = \int dF = \epsilon_0 \,\mathrm{Re} \int_0^\zeta \{-2\,\mathrm{Im}\, DC^* - i(|D|^2 - |C|^2) + 2|D + C|^2 \zeta'^*\} d\zeta', \tag{A6}$$

using Eq. (A4) to express $G_j$ and $H_j$. Since the integrand is linear in $\zeta'$, the integral is easily evaluated to give

$$F = \epsilon_0(|D|^2 - |C|^2)\mathrm{Im}\,\zeta - 2\epsilon_0(\mathrm{Im}\, DC^*)\mathrm{Re}\,\zeta + \epsilon_0|D+C|^2|\zeta|^2. \tag{A7}$$

Here, formally, the first term is exactly the "radiation pressure," the second, the "dipole force" summed over all the particles due to an electric field $De^{ikx}+C^{-ikx}$, and all the nonlinear "multiple scattering" corrections are in the third term. Bear in mind, however, that some of the nonlinearity is "hidden" in $D$, which is related to the incident amplitude $B$ nonlinearly in $\zeta$:

$$D = \frac{1}{1-i\zeta}(i\zeta C + B). \tag{A8}$$

Substitution of this relation into Eq. (A7) yields

$$F = 2\frac{I_0 - I_1}{c}\frac{\mathrm{Im}\,\zeta}{|1-i\zeta|^2} - 4\frac{\sqrt{I_0 I_1}}{c}\frac{\mathrm{Re}\,\zeta}{|1-i\zeta|^2}\sin(2kx+\varphi) + 2\frac{I_0 - I_1}{c}\frac{|\zeta|^2}{|1-i\zeta|^2}, \tag{A9}$$

with the incident intensities $I_0=\frac{1}{2}\epsilon_0 c|B|^2$ and $I_1=\frac{1}{2}\epsilon_0 c|C|^2$, and the relative phase $\varphi=\arg B-\arg C$. This is identical to the formula (22) derived via the Maxwell stress tensor in Sec. II.

## APPENDIX B: SYMMETRICALLY PUMPED LATTICE

We have derived the analytical form of the force matrix **D** in Sec. V, and we could describe the dynamics of a symmetrically pumped lattice simply by taking the limit $\mathcal{A}\to 0$ of the formulas. This seems to make perfect sense, as the final formulas, i.e., the force matrix **D** (62), eigenmodes of vibration $\mathbf{v}_b$ (67), and the corresponding eigenvalues $z_b$ (68) have well defined limiting values for $I_1\to I_0$. However, it is quite disturbing that the derivation of these formulas does not work for $I_0=I_1$. If $\mathcal{P}=1$, the two vectors **u** (49) and **w** (51) are parallel and thus they do not subtend a basis (not even a nonorthogonal one). We therefore fill a gap in this section by deriving the formulas for symmetric pumping. Reassuringly, the same results are found as by directly taking the limit.

In the symmetric pumping case the $2\times 2$ transfer matrix **M** only has one eigenvector **u** ($=e^{-i\chi}\mathbf{w}$). This awkward situation arises because for symmetric pumping $\Theta=\pi$, thus $\mathrm{tr}\,\mathbf{M}=2$ [see Eq. (19)], and then the characteristic equation has a single eigenvalue 1 with a multiplicity of 2. Although such matrices are not diagonalizable, their functions can still be computed efficiently using the Jordan form. In-

stead of just referring the reader this general recipe, we here give the detailed calculation.

Since we have a single eigenvector $\mathbf{u}$, it is useful to take a second vector $\mathbf{z}$ orthogonal to it

$$\mathbf{u} = \frac{1}{\sqrt{2}}\begin{pmatrix} 1 \\ e^{-i\chi} \end{pmatrix}, \quad \mathbf{z} = \frac{1}{\sqrt{2}}\begin{pmatrix} 1 \\ -e^{-i\chi} \end{pmatrix}. \tag{B1}$$

Note that with these definitions $\mathbf{u}$ and $\mathbf{z}$ provide an orthonormal basis. Substitution of $\chi$ leads to

$$\text{red detuning, } \zeta > 0: \quad \mathbf{u} = \frac{e^{-i\tan^{-1}\zeta}}{\sqrt{2}\sqrt{1+\zeta^2}}\begin{pmatrix} 1+i\zeta \\ 1-i\zeta \end{pmatrix},$$

$$\mathbf{z} = \frac{e^{-i\tan^{-1}\zeta}}{\sqrt{2}\sqrt{1+\zeta^2}}\begin{pmatrix} 1+i\zeta \\ -1+i\zeta \end{pmatrix}, \tag{B2a}$$

$$\text{blue detuning, } \zeta < 0: \quad \mathbf{u} = \frac{1}{\sqrt{2}}\begin{pmatrix} 1 \\ -1 \end{pmatrix}, \quad \mathbf{z} = \frac{1}{\sqrt{2}}\begin{pmatrix} 1 \\ 1 \end{pmatrix}. \tag{B2b}$$

It can easily be checked by direct calculation that a decomposition analogous to Eq. (20) can be given:

$$\mathbf{M} = -1 + 2i|\zeta|\mathbf{u}\circ\mathbf{z}^{\dagger}, \tag{B3}$$

and this can be used directly to show that for any $n \in \mathbb{N}$,

$$\mathbf{M}^n\mathbf{u} = (-1)^n\mathbf{u}, \tag{B4a}$$

$$\mathbf{M}^n\mathbf{z} = (-1)^n\mathbf{z} + n(-1)^{n-1}2i|\zeta|\mathbf{u}. \tag{B4b}$$

Mirror reflection of $\mathbf{u}$ along $x$ is now simpler then for the asymmetric pumping case. We have

$$\zeta\boldsymbol{\sigma}\mathbf{P}(d)\mathbf{u} = -|\zeta|\mathbf{u}. \tag{B5}$$

Perturbation of the optical lattice (infinitesimal displacement of the $l$th cloud by $\xi \to 0$) given in Eq. (53) still only affects the outgoing modes, but now for $a^{(l)}$ and $b^{(l)}$ of Eq. (53) we have

$$\begin{pmatrix} a^{(l)} \\ 0 \end{pmatrix} = a_u^{(l)}\mathbf{u} + a_z^{(l)}\mathbf{z}, \quad a_u^{(l)} = a_z^{(l)} = \frac{a}{\sqrt{2}}, \tag{B6a}$$

$$\begin{pmatrix} 0 \\ b \end{pmatrix} = b_u^{(l)}\mathbf{u} + b_z^{(l)}\mathbf{z}, \quad b_u^{(l)} = -b_z^{(l)} = \frac{be^{i\chi}}{\sqrt{2}}. \tag{B6b}$$

Using these decompositions, to first order in the small parameter $\varepsilon = k\xi$, Eq. (53) can be written as

$$\frac{1}{\sqrt{2}}a^{(l)}(\mathbf{u}+\mathbf{z}) = \frac{b^{(l)}e^{i\chi}}{\sqrt{2}}(-1)^N[(1+2N|\zeta|i)\mathbf{u}-\mathbf{z}] - 2(-1)^N|\zeta|\mathbf{u}. \tag{B7}$$

The $\mathbf{u}$ and $\mathbf{z}$ components of this equation together give

$$b^{(l)} = \frac{\sqrt{2}|\zeta|e^{-i\chi}}{1+N|\zeta|i} \tag{B8}$$

Having obtained $b$, we can use the transfer matrices to find the mode amplitudes $A_j$ and $B_j$ inside the structure from right to left successively:

$$j > l: \quad \begin{pmatrix} A_j \\ B_j \end{pmatrix} \neq \mathcal{E}_0\mathbf{M}^{N-j+1}\left[\mathbf{u} + \varepsilon\frac{be^{i\chi}}{\sqrt{2}}(\mathbf{u}-\mathbf{z})\right]$$
$$= (-1)^{(N-j+1)}\mathcal{E}_0\Bigg(\mathbf{u} + \varepsilon\frac{be^{i\chi}}{\sqrt{2}} \times\{[1+(N-j+1)2|\zeta|i]\mathbf{u}-\mathbf{z}\}\Bigg). \tag{B9}$$

Now due to $\mathbf{u}^{\dagger}\cdot\mathbf{z}=0$, it is easier to compute the sum of the mode intensities to first order in $\varepsilon$:

$$\frac{|A_j|^2+|B_j|^2}{|E_0|^2} = 1 + 2\varepsilon\ \mathrm{Re}\frac{be^{i\chi}}{\sqrt{2}}[1+(N-j+1)2|\zeta|i], \tag{B10}$$

$$j \leq l: \quad \begin{pmatrix} A_j \\ B_j \end{pmatrix} \neq \mathcal{E}_0[\mathbf{M}^{N-j+1} - 2\varepsilon\zeta\mathbf{M}^{l-j}\boldsymbol{\sigma}\mathbf{P}(d)\mathbf{M}^{N-l}] \times\left[\mathbf{u} + \epsilon\frac{be^{i\chi}}{\sqrt{2}}(\mathbf{u}-\mathbf{z})\right]$$
$$= (-1)^{(N-j+1)}\mathcal{E}_0\Bigg(\mathbf{u} + \varepsilon\frac{be^{i\chi}}{\sqrt{2}} \times\{[1+(N-j+1)2|\zeta|i]\mathbf{u}-\mathbf{z}\} - 2\varepsilon|\zeta|\mathbf{u}\Bigg). \tag{B11}$$

To first order in $\varepsilon$ we now have

$$\frac{|A_j|^2+|B_j|^2}{|E_0|^2} = 1 + 2\varepsilon\ \mathrm{Re}\frac{be^{i\chi}}{\sqrt{2}}[1+(N-j+1)2|\zeta|i] - 4\varepsilon|\zeta|. \tag{B12}$$

Having found the intensities, we now only need to subtract them to find the force (21):

$$D_{jl} = \frac{k}{\varepsilon}F_j = \frac{\varepsilon_0}{2}\left[2\ \mathrm{Re}\left(\frac{be^{i\chi}}{\sqrt{2}}2|\zeta|i\right) - \delta_{lj}4|\zeta|\right]2k|E_0|^2$$
$$= \beta\left(\frac{N\zeta^2}{1+N^2\zeta^2} - \delta_{lj}\right) \tag{B13}$$

with $\beta = 8k|\zeta|I_0/c = 4k|\zeta|\epsilon_0|E_0|^2$ as in Eq. (37). This is identical to Eq. (63), found in Sec. V as the limit of the full result Eq. (62) as $|E_1| \to |E_0|$.

[1] For a review of the optical lattices, see P. Jessen and I. Deutsch, Adv. At., Mol., Opt. Phys. **37**, 95 (1996).
[2] I. Bloch, Nat. Phys. **1**, 23 (2005).
[3] G. Campbell *et al.*, Science **313**, 649 (2006).
[4] W. Hofstetter, J. I. Cirac, P. Zoller, E. Demler, and M. D. Lukin, Phys. Rev. Lett. **89**, 220407 (2002).
[5] G. K. Brennen, C. M. Caves, P. S. Jessen, and I. H. Deutsch, Phys. Rev. Lett. **82**, 1060 (1999).
[6] M. Takamoto, F.-L. Hong, R. Higashi, and H. Katori, Nature (London) **435**, 321 (2005).
[7] P. Domokos and H. Ritsch, J. Opt. Soc. Am. B **20**, 1098 (2003).
[8] P. Maunz *et al.*, Nature (London) **428**, 50 (2004).
[9] S. Gigan *et al.*, Nature (London) **444**, 67 (2006).
[10] O. Arcizet *et al.*, Nature (London) **444**, 71 (2006).
[11] D. Kleckner and D. Bouwmeester, Nature (London) **444**, 75 (2006).
[12] I. H. Deutsch, R. J. C. Spreeuw, S. L. Rolston, and W. D. Phillips, Phys. Rev. A **52**, 1394 (1995).
[13] G. Birkl, M. Gatzke, I. H. Deutsch, S. L. Rolston, and W. D. Phillips, Phys. Rev. Lett. **75**, 2823 (1995).
[14] M. Weidemüller, A. Görlitz, T. W. Hänsch, and A. Hemmerich, Phys. Rev. A **58**, 4647 (1998).
[15] T. Elsasser, B. Nagorny, and A. Hemmerich, Phys. Rev. A **69**, 033403 (2004).
[16] J. Klinner, M. Lindholdt, B. Nagorny, and A. Hemmerich, Phys. Rev. Lett. **96**, 023002 (2006).
[17] J. K. Asboth, P. Domokos, and H. Ritsch, Phys. Rev. A **70**, 013414 (2004).
[18] P. Domokos and H. Ritsch, Phys. Rev. Lett. **89**, 253003 (2002).
[19] J. K. Asboth, P. Domokos, H. Ritsch, and A. Vukics, Phys. Rev. A **72**, 053417 (2005).
[20] A. T. Black, H. W. Chan, and V. Vuletić, Phys. Rev. Lett. **91**, 203001 (2003).
[21] J. Javaloyes, M. Perrin, G. L. Lippi, and A. Politi, Phys. Rev. A **70**, 023405 (2004).
[22] G. R. M. Robb, N. Piovella, A. Ferraro, R. Bonifacio, Ph. W. Courteille, and C. Zimmermann, Phys. Rev. A **69**, 041403 (2004).
[23] S. Slama, S. Bux, G. Krenz, C. Zimmermann, and Ph. W. Courteille, Phys. Rev. Lett. **98**, 053603 (2007).
[24] G. R. M. Robb and W. J. Firth, Phys. Rev. Lett. **99**, 253601 (2007).
[25] M. M. Burns, J.-M. Fournier, and J. A. Golovchenko, Phys. Rev. Lett. **63**, 1233 (1989).
[26] W. Singer, M. Frick, S. Bernet, and M. Ritsch-Marte, J. Opt. Soc. Am. B **20**, 1568 (2003).
[27] S. A. Tatarkova, A. E. Carruthers, and K. Dholakia, Phys. Rev. Lett. **89**, 283901 (2002).
[28] J. Ng, Z. F. Lin, C. T. Chan, and P. Sheng, Phys. Rev. B **72**, 085130 (2005).
[29] D. Maystre and P. Vincent, J. Opt. A, Pure Appl. Opt. **8**, 1059 (2006).
[30] T. M. Grzegorczyk, B. A. Kemp, and J. A. Kong, Phys. Rev. Lett. **96**, 113903 (2006).
[31] V. Karásek and P. Zemánek, J. Opt. A, Pure Appl. Opt. **9**, S215 (2007).
[32] C. Cohen-Tannoudji, in *Fundamental Systems in Quantum Optics, Proceedings of the Les Houches Summer School, Session LIII*, edited by J. Dalibard, J.-M. Raimond, and J. Zinn-Justin (North-Holland, Amsterdam, 1992), pp. 1–164.
[33] For Im $\Theta \neq 0$, we have $|m_-| < 1 < |m_+|$ or $|m_+| < 1 < |m_-|$. Multiplication of many transfer matrices is therefore numerically ill conditioned: Important variables can take on different orders of magnitude and are then added together. In numerical calculations in mesoscopic physics it can therefore be advisable to fall back to the scattering matrix. For the transfer matrices in our case, usually $|\mathrm{Im}\,\Theta|$ is of the order of Im $\zeta$, and as normally $|N\,\mathrm{Im}\,\zeta| < 1$ (required so that absorption does not alter the asymmetry too much throughout the sample), these numerical issues do not concern us.
[34] D. McGloin, A. E. Carruthers, K. Dholakia, and E. M. Wright, Phys. Rev. E **69**, 021403 (2004).
[35] D. Meiser and P. Meystre, Phys. Rev. A **73**, 033417 (2006).
[36] D. Meiser and P. Meystre, Phys. Rev. A **74**, 065801 (2006).
[37] J. K. Asboth and P. Domokos, Phys. Rev. A **76**, 057801 (2007).
[38] M. I. Antonoyiannakis and J. B. Pendry, Phys. Rev. B **60**, 2363 (1999).
[39] Note that the fluctuations of this force, arising from the spontaneous emission accompanying absorption, lead to a heating of the cloud, which limits the time scale of experiments. We come back to this issue in Sec. VII.
[40] A. Ashkin, Phys. Rev. Lett. **24**, 156 (1970).
[41] The color coding and slashed lines denoting the regimes of stability come in fact from the analytical calculations detailed in Sec. V, and not directly from simulations themselves (the computational cost is only linear with $N$, but simulations with $N=10^6$ are still impractical). Therefore they correspond to stability with respect to infinitesimal perturbations. As such, they have been checked via simulation and seen to be correct several times, as illustrated in the examples in Figs. 9 and 10.
[42] In fact, the derivation of Eq. (62) is not valid for symmetric pumping, and therefore one must use a different approach. However, as we show in Eq. (A9), a mathematically sound procedure also leads to Eq. (63).
[43] R. A. Simha and S. Ramaswamy, Phys. Rev. Lett. **83**, 3285 (1999).
[44] T. Beatus, T. Tlusty, and R. Bar-Ziv, Nat. Phys. **2**, 743 (2006).
[45] T. Beatus, R. Bar-Ziv, and T. Tlusty, Phys. Rev. Lett. **99**, 124502 (2007).